RABI FORMULA ANALOGS FOR DOUBLE AND TRIPLE PHOTON ABSORPTION PROCESSES

by

Michael Daniel Burrows

A Thesis Submitted to the Faculty of the

DEPARTMENT OF CHEMISTRY

In Partial Fulfillment of the Requirements
For the Degree of

MASTER OF SCIENCE

In the Graduate College

THE UNIVERSITY OF ARIZONA

1 9 7 5

STATEMENT BY AUTHOR

This thesis has been submitted in partial fulfillment of requirements for an advanced degree at The University of Arizona and is deposited in the University Library to be made available to borrowers under rules of the Library.

Brief quotations from this thesis are allowable without special permission, provided that accurate acknowledgment of source is made. Requests for permission for extended quotation from or reproduction of this manuscript in whole or in part may be granted by the head of the major department or the Dean of the Graduate College when in his judgment the proposed use of the material is in the interests of scholarship. In all other instances, however, permission must be obtained from the author.

SIGNED: Michael D. Benson

APPROVAL BY THESIS DIRECTOR

This thesis has been approved on the date shown below:

W. R. Salzman — 22 Jan 75

W. R. SALZMAN
Associate Professor of Chemistry

Date

ACKNOWLEDGMENTS

The author wishes to express his sincere appreciation and gratitude to Professor W. R. Salzman, his thesis advisor, for providing the initial theoretical impetus essential to the calculations presented in this thesis. In addition to providing the theoretical groundwork on which these calculations were based, Professor Salzman allowed the author considerable freedom in the choice of systems to which the theory could be applied, enabling the author to enhance his ability for independent research.

The author is also indebted to Doctors W. B. Miller and L. S. Forster, his committee members, for the time and patience they expended in both the perusal of the author's thesis and in participating in the author's oral examination.

The author wishes to express his admiration and appreciation to Ms. Kristi Riggins whose patience and understanding provided the personal sustenance so essential to any undertaking of this magnitude. It is appropriate, then, that this work be dedicated to her.

The financial support received from the Department of Chemistry through teaching assistantships is gratefully acknowledged.

TABLE OF CONTENTS

LIST OF TABLES

LIST OF TABLES--Continued

LIST OF TABLES--Continued

LIST OF TABLES--Continued

LIST OF ILLUSTRATIONS

LIST OF ILLUSTRATIONS--Continued

ABSTRACT

Time evolution operator theory has been applied to test the validity of previously derived Rabi formula analogs for double and triple photon absorption processes. The time evolution operator technique involves numerical integration of the differential equation for the time evolution operator in the interaction representation using a rigid rotor model system. The Rabi formula analogs for double and triple photon absorption derived by Oka and Shirley, respectively, break down when nearest neighbor energy levels not directly involved in the multiple photon absorption process were included in the calculation. In addition, the level shift interactions for single, double, and triple photon absorption processes were found to extend only as far as the nearest neighbor energy levels.

CHAPTER I

INTRODUCTION

The advent of high intensity lasers has brought about a renewed interest in both the theoretical and experimental aspects of multiple photon processes. Recent experiments employing microwave-infrared two photon spectroscopy have in effect made laser radiation sources tunable by the "addition" of a microwave frequency to an infrared frequency using a double photon transition (1). The technique of high-resolution double photon spectroscopy also looks promising (2-5).

Although the original double photon calculations performed by Goeppert-Mayer (6) employed a quantized radiation field, the techniques of semiclassical radiation theory have been applied with considerable accuracy to multiple photon transitions. Despite the ultimate limitations of semiclassical radiation theory in predicting spontaneous emission rates, for example, its value as a predictive tool cannot be underestimated. Several recent experiments using high-resolution double photon spectroscopy have derived their inspiration from essentially semiclassical theories (7). Quantum electrodynamics is the ultimate theory at present, but the intuitive preference remains the

electromagnetic field of Maxwell's equations, rather than the creation and annihilation of photons. In essence, semi-classical radiation theory is sufficient for most problems dealing with stimulated emission and absorption.

Time-evolution operator theory has been used previously by various authors to determine transition probabilities for multiple photon absorption (8) and to derive the Rabi formula for a general quantum system of more than two levels (9). In this thesis time evolution operator calculations will be performed on a specific molecular model system to test the validity of previously derived expressions for the time-dependent transition probability for double photon and triple photon absorption. In essence, the time evolution operator calculations performed in this thesis involve numerical integration of the differential equation for the time evolution operator in the interaction representation. Once the differential equation has been integrated by an iterative procedure up to time $t=\tau$, the period of the driving field frequency, the relation $T(n\tau)=(T(\tau))^n$ can then be applied, where $T(t)$ is the time evolution operator in the Schroedinger representation. The pertinent theory and details of the iterative procedure are outlined in Chapter II. In Chapter III the general requirements for double and triple photon absorption are discussed and the parameters of the CD_3CN model system specified. Chapter IV gives the results of the time evolution operator

calculations for double and triple photon absorption, and compares them with the results predicted by the relations of Oka and Shimizu (10) and Shirley (11), respectively. The changes in the net level shift factors and resonance frequencies produced by including additional energy levels not directly involved in the double and triple photon transitions are particularly noteworthy. The feasibility of double and triple photon absorption experiments in the infrared and visible spectral regions is discussed in Chapter VI.

Time evolution operator calculations were also performed for systems of three to six equally spaced levels and for three level systems with almost equally spaced levels. For the latter three level systems both the Rabi formula and the corrected version of Oka's formula were found to break down. The results of these calculations are given in Chapter V.

CHAPTER II

TIME EVOLUTION OPERATOR THEORY

If $|a,t_o\rangle$ specifies the state of a physical system at time t_o in the Schroedinger representation, the time evolution operator $T(t,t_o)$ yields the state of the system at some later time t through the operator equation

$$|a,t\rangle = T(t,t_o) \mid a,t_o\rangle. \qquad \text{(II-1)}$$

The use of T to denote the time evolution operator does not imply any connection with the T-matrix of scattering theory. From Equation (II-1),

$$T(t,t) = 1 \qquad \text{(II-2)}$$

and

$$T(_2,t_o) = T(t_2,t_1)\ T(t_1,t_o) \qquad \text{(II-3)}$$

follow.

The form of the time evolution operator is determined by the Hamiltonian of the system through the operator equation

$$i\hbar \frac{d}{dt} T(t,t_o) = H(t)\ T(t,t_o) \qquad \text{(II-4)}$$

which follows from Equation (II-1) and the Schroedinger equation.

$$i\hbar \frac{d}{dt} |a,t\rangle = H(t)|a,t\rangle$$

since H(t) is always Hermitian, $T(t,t_o)$ is unitary (12).

Determination of the form of $T(t,t_o)$ is often made easier by a transformation into the interaction representation. The equation of motion for the state vector $|\psi(t)\rangle$ in the Schroedinger representation is

$$i\hbar \frac{d}{dt} |\psi(t)\rangle = (H_o+V)|\psi(t)\rangle, \qquad \text{(II-5)}$$

where H_o is the time-independent portion of the total Hamiltonian given by $H_o + V$, and V may depend on time. If the state vector in the interaction representation is taken as

$$|\psi_I(t)\rangle = \exp(i H_o t/\hbar)|\psi(t)\rangle, \qquad \text{(II-6)}$$

differentiating $|\psi_I(t)\rangle$ yields

$$i\hbar \frac{d}{dt} |\psi_I(t)\rangle = V_I(t)|\psi_I(t)\rangle \qquad \text{(II-7)}$$

where

$$V_I(t) = \exp(i H_o t/\hbar) V \exp(-i H_o t/\hbar). \qquad \text{(II-8)}$$

Hence, the time-development of $|\psi_I(t)\rangle$ depends on the time-dependent portion of the total Hamiltonian. If the physical system consists of an atom in a radiation field, H_o becomes the unperturbed Hamiltonian of the atom and V(t) represents the interaction between the quantized atom and the classical radiation field, in the dipole approximation. Since H_o is time independent, the transformation into the interaction representation is unitary. The time evolution operator in the interaction representation takes the form

$$|\psi_I(t)\rangle = U(t,t_o)\,|\psi_I(t_o)\rangle. \qquad \text{(II-9)}$$

The transformation connecting $T(t,t_o)$ and $U(t,t_o)$ can be found by considering

$$|\psi_I(t)\rangle = U(t,t_o)\,|\psi_I(t_o)\rangle$$

$$\exp(i\,H_o t/\hbar)\,|\psi(t)\rangle = U(t,t_o)\,\exp(i\,H_o t_o/\hbar)\,|\psi(t_o)\rangle$$

$$\exp(i\,H_o t/\hbar)\;T(t,t_o)\,|\psi(t_o)\rangle =$$

Hence,

$$U(t,t_o) = \exp(i\,H_o t/\hbar)\;T(t,t_o)\;\exp(-i\,H_o t_o/\hbar), \qquad \text{(II-10)}$$

and since $T(t,t_o)$ is unitary, $U(t,t_o)$ must also be unitary.

The differential equation for $U(t,t_o)$ can be found by taking the time derivative of the transformed time evolution operator given by Equation (II-10).

$$\frac{d}{dt}\,U(t,t_o) = (i\,H_o/\hbar)U(t,t_o)$$

$$+\,\exp(i\,H_o t/\hbar)\left(\frac{d}{dt}\,T(t,t_o)\right)\exp(-i\,H_o t_o/\hbar)$$

$$= (i\,H_o/\hbar)U(t,t_o)$$

$$+\,\exp(i\,H_o t/\hbar)\,(H_o T(t,t_o)/i\hbar)\,\exp(-i\,H_o t_o/\hbar)$$

$$+\,\exp\,(i\,H_o t/\hbar)\,\frac{V(t)T(t,t_o)}{i\,\hbar}\,\exp(-i\,H_o t_o/\hbar)$$

$$= (1/i\hbar)\;V_I(t)U(t,t_o),$$

and

$$i\hbar\,\frac{d}{dt}\,U(t,t_o) = V_I(t)U(t,t_o), \qquad \text{(II-11)}$$

subject to the initial condition

$$U(t_o,t_o) = 1. \qquad \text{(II-12)}$$

From Equation (II-10) it can also be shown that

$$U(t,t") = U(t,t')U(t',t"). \qquad \text{(II-13)}$$

The differential equation for $U(t,t_o)$ is usually cast as the integral equation

$$U(t,t_o) = 1 - \frac{i}{\hbar}\int_{t_o}^{t} V_I(t')U(t',t_o)\,dt'. \qquad \text{(II-14)}$$

This equation can be used as the starting point for a self-consistent, successive approximation technique. First $U(t_o,t_o) = 1$ is substituted under the integral; the approximate $U(t,t_o)$ obtained is substituted again in the integrand, and the process repeated. The result of repeated iterations is a power series in V:

$$U(t,t_o) = 1 - \frac{i}{\hbar}\int_{t_o}^{t} V_I(t')dt' + \left(\frac{-i}{\hbar}\right)^2 \int_{t_o}^{t} V_I(t') \cdot \int_{t_o}^{t'} V_I(t")dt'dt" + \ldots \qquad \text{(II-15)}$$

In a similar manner Equations (II-4) and (II-2) can be used to obtain

$$T(t,t_o) = 1 - \frac{i}{\hbar}\int_{t_o}^{t} H(t')T(t',t_o)\,dt' \qquad \text{(II-16)}$$

in the Schroedinger representation. Application of the iterative technique used above yields

$$T(t,t_o) = 1 - \frac{i}{\hbar}\int_{t_o}^{t} H(t')\,dt + \left(\frac{-i}{\hbar}\right)^2 \int_{t_o}^{t} H(t') \cdot \int_{t_o}^{t} H(t'')\,dt''dt' + \ldots \qquad \text{(II-17)}$$

in the Schroedinger representation. The main utility of (II-17) in this paper lies in the proof that $T(n\tau,0) = (T(\tau, 0))^n$ under certain conditions.

From the power series for $T(t,t_o)$ the result

$$T(n\tau, 0) = (T(\tau, 0))^n \qquad \text{(II-18)}$$

can be shown to hold, provided $V(t)$ is periodic in time with period τ such that

$$V(t + \tau) = V(t). \qquad \text{(II-19)}$$

For example, if $V(t) = \mu E_o \sin(wt)$, $\tau = 2\pi/w$. Note that t_o has been taken as zero for convenience. The total time-dependent Hamiltonian is assumed to have the form

$$H(t) = H_o + V(t) \qquad \text{(II-20)}$$

so that the periodicity of $V(t)$ yields

$$H(t + \tau) = H_o + V(t + \tau) = H_o + V(t) = H(t) \qquad \text{(II-21)}$$

To verify Equation (II-18), subject to the restriction (II-19), a proof by induction shall be used. For

$$T(2\tau, \tau)\ T(\tau, 0) = T(2\tau, 0)$$

Equation (II-17) yields

$$T(2\tau,\tau) = 1 + \frac{1}{i\hbar}\int_{\tau}^{2\tau} H(t')dt' + \left(\frac{1}{i\hbar}\right)^2 \cdot$$

$$\int_{\tau}^{2\tau} H(t') \int_{\tau}^{t'} H(t")dt"dt' + \ldots$$

Changing to the new set of variables,

$$s' = t' - \tau$$

$$s" = t" - \tau$$

$$\ldots$$

$$s^{(n)} = t^{(n)} - \tau,$$

yields,

$$T(2\tau, \tau) = 1 + \frac{1}{i\hbar}\int_{0}^{\tau} H(s' + \tau)ds' + \left(\frac{1}{i\hbar}\right)^2 \cdot$$

$$\int_{0}^{\tau} H(s' + \tau) \int_{0}^{s'} H(s" + \tau)ds"ds' + \ldots,$$

which the periodicity of H(t) reduces to:

$$T(2\tau, \tau) = 1 + \frac{1}{i\hbar}\int_{0}^{\tau} H(s')ds' + \left(\frac{1}{i\hbar}\right)^2 \cdot$$

$$\int_{0}^{\tau} H(s') \int_{0}^{s'} H(s")ds"ds' + \ldots = T(\tau, 0),$$

and $T(2\tau, \tau)T(\tau, 0) = (T(\tau, 0))^2 = T(2\tau, 0)$.

Assuming that $T(n\tau, 0) = (T(\tau, 0))^n$, it must now be demonstrated that $T((n + 1)\tau, 0) = (T(\tau, 0))^{n+1}$. From Equation (II-3),

$$T((n+1)\tau, 0) = T((n+1)\tau, n\tau)T(n\tau, 0),$$

and the integral equation expansion yields

$$T((n+1)\tau,\ n\tau) = 1 + \frac{1}{i\hbar}\int_{n\tau}^{(n+1)\tau} H(t')dt'$$

$$+ \left(\frac{1}{i\hbar}\right)^2 \int_{n\tau}^{(n+1)\tau} H(t') \int_{n\tau}^{t'} H(t")dt"dt' + \ldots .$$

With the change of variables,

$$s' = t' - n\tau$$

$$s" = t" - n\tau$$

$$\ldots$$

$$s^{(m)} = t^{(m)} - n\tau$$

$$T((n+1)\ \tau,\ n\tau) = 1 + \frac{1}{i\hbar}\int_0^{\tau} H(s'+n\tau)ds'$$

$$+ \left(\frac{1}{i\hbar}\right)^2 \int_0^{\tau} H(s'+n\tau) \cdot$$

$$\int_0^{s'} H(s" + n\ \tau)ds"ds' + \ldots,$$

which the periodicity of H(t) reduces to:

$$T((n+1)\ \tau,\ n\ \tau) = 1 + \frac{1}{i\hbar}\int_0^{\tau} H(s')ds'$$

$$+ \left(\frac{1}{i\hbar}\right)^2 \int_0^{\tau} H(s') \int_0^{s'} H(s")ds"ds' + \ldots = T(\tau,\ 0).$$

Hence, $T((n+1)\ \tau,0) = (T(\tau,\ 0))^{n+1}$, and Equation (II-18) is verified.

The differential equation for $U(t,t_o)$ can now be used in conjunction with a Taylor series expansion of

$U(t,t_o = 0)$ to obtain a numerical iteration procedure for the evaluation of $U(t = \tau, 0)$. It is assumed that $V(t)$ is periodic with period τ so that the iterative process described below can be terminated at $t = \tau$ and Equation (II-18) applied once $U(\tau, 0)$ has been transformed back into the Schroedinger representation. It is also assumed that the initial or reference time for the "switch-on" of the perturbation $V(t)$ is $t_o = 0$.. Hence, $U(t,t_o) = U(t,0) = U(t)$ and $t_o = 0$ will be suppressed for notational convenience. For the purposes of this paper, the transient response of the system after the "switch-on" of $V(t)$ will be ignored.

For time increments $\delta << \tau$,

$$U(t+\delta) = U(t) + (\delta)\frac{d}{dt} U(t) + \frac{(\delta)^2}{2!} \frac{d^2}{dt^2} U(t) + \ldots \quad \text{(II-22)}$$

If this series is teriminated at first order,

$$U(t + \delta) \cong U(t) + \delta\frac{d}{dt} U(t),$$

where

$$\frac{d}{dt} U(t) = \frac{1}{i\hbar} V_I(t)\ U(t).$$

Hence,

$$U(t + \delta) \cong (1+(\delta/i\hbar)V_I(t))\ U(t). \quad \text{(II-23)}$$

Since $U(0) = 1$, for $t = 0$ and $\delta = \tau/n$,

$$U(\delta) \cong (1+ \frac{\delta}{i\hbar} V_I(0))\ U(0) = (1+ \frac{\delta}{i\hbar} V_I(0)).$$

Equation (II-23) can now be applied repeatedly to yield the

iterative process

$$U(2\cdot\delta) \cong (1 + \frac{\delta}{i\hbar} V_I(\delta))U(\delta)$$

$$U(3\cdot\delta) \cong (1 + \frac{\delta}{i\hbar} V_I(2\cdot\delta))U(2\cdot\delta)$$

$$\cdots$$

$$U(n\cdot\delta) \cong (1 + \frac{\delta}{i\hbar} V_I((n-1)\cdot\delta))U((n-1)\cdot\delta).$$

The iterative process is carried out for n large (usually 1000) and terminated when $n\cdot\delta = \tau$. In essence, the differential equation for U(t) has been numerically integrated from t = 0 to t = τ. Once U(τ) is known, transforming back into the Schroedinger representation using Equation (II-10) with $t_o = 0$ yields T(τ). For times t > τ, but with t/τ integral, the relation $T(m\tau) = (T(\tau))^m$ can then be applied. For perturbations of the form $V(t) = \mu E_o \sin(w\cdot t)$ where the driving field is resonant with the atomic or molecular system specifying H_o and single photon absorption occurs, and transition rate, hereafter referred to as the Rabi frequency, is much slower than the driving field frequency. For two or three photon absorption the transition rates are slower still, so the restriction to times that are integer multiples of $\tau = 2\pi/w$ does not limit the utility of the technique in practice.

If T(t), where $t = a\tau + b$, $b < \tau$, and a is an integer, is required, Equation (II-18) can be applied to find T(a τ). T(a τ) must then be transformed to U(a τ) and the iterative procedure above then used to

generate $U(t = a\tau + b)$. Equation (II-10) can then be used to generate $T(a\tau + b)$.

If the series given by (II-22) is terminated at second order,

$$U(t+\delta) \cong (1 + \frac{\delta}{i\hbar} V_I(t))U(t) + (\delta^2/2!)\frac{d^2}{dt^2} U(t)$$

where

$$\frac{d^2}{dt^2} U(t) = \frac{1}{i\hbar} \frac{d}{dt} (V_I(t)U(t))$$

$$= \frac{1}{i\hbar} ((\frac{d}{dt} V_I(t))U(t)+V_I(t)(\frac{d}{dt}U(t)))$$

$$= \frac{1}{i\hbar} (V_I'(t)U(t) + V_I(t)\frac{1}{i\hbar} V_I(t)U(t))$$

$$= (\frac{1}{i\hbar} V_I'(T) + (\frac{1}{i\hbar})^2(V_I(t)^2))U(t),$$

and Equation (II-10) has been invoked. Hence,

$$U(t+\delta) \cong (1+ \frac{\delta}{i\hbar} V_I(t) + \frac{1}{i\hbar} \frac{\delta^2}{2!} V_I'(t)$$

$$+ (\frac{\delta}{i\hbar})^2 \frac{1}{2!} (V_I(t))^2)U(t), \qquad \text{(II-24)}$$

to second order. The iterative process for the second order expression is analogous to that for the first order. Since $U(0) = 1$, for $t = 0$ and $\delta = \tau/n$,

$$U(\delta) \cong (1+ \frac{\delta}{i\hbar} V_I(0) + \frac{1}{i\hbar} \frac{\delta^2}{2!} V_I'(0)$$

$$+ (\frac{\delta}{i\hbar})^2 \frac{1}{2!} (V_I(0))^2)U(0)$$

and Equation (II-24) can now be applied repeatedly to yield the iterative process

$$U(2\delta) \cong (1+ \frac{\delta}{i\hbar} V_I(\delta) + \frac{1}{i\hbar} \frac{\delta^2}{2!} V_I'(\delta) + (\frac{\delta}{i\hbar})^2 \frac{1}{2!} (V_I(\delta))^2) U(\delta)$$

$$\cdots$$

$$U(n\delta) \cong (1+ \frac{\delta}{i\hbar} V_I((n-1)\delta) + \frac{1}{i\hbar} \frac{\delta^2}{2!} V_I'((n-1)\delta) + (\frac{\delta}{i\hbar})^2 \frac{1}{2!}(V_I((n-1)\delta))^2) U(n-1)\delta).$$

As for the first-order case, the iterative process is carried out for n large and terminated when $n\delta = \tau$. Again, the differential equation for U(t) has been, in essence, numerically integrated from t = 0 to $t = \tau$. For times $t > \tau$, but with t/τ an integer, the relation $T(m\tau) = (T(\tau))^m$ can now be applied.

Since the time evolution operator yields the evolution of a quantum system in time, it is ideal for calculating transition rates. Under the influence of the monochromatic, coherent driving field,

$$E = E_o \sin(w \cdot t), \qquad \text{(II-25)}$$

the perturbation on the atomic or molecular system specified by H_o becomes, in the dipole approximation,

$$V(t) = \mu E_o \sin(w \cdot t). \qquad \text{(II-26)}$$

Once T(t) has been determined, $|\langle a|T(t)|b\rangle|^2$ yields the probability for the transition $b \to a$ at time t, where T(t) is obtained from (II-18) in conjunction with the iterative

process based on either (II-23) or (II-24). It should be noted that the time evolution operator so calculated does not include any effects attributable to a quantized radiation field, such as spontaneous emission. Thus the multiple photon calculations performed are in the domain of semi-classical radiation theory, and $|\langle a|T(t)|b\rangle|^2$ accounts for stimulated emission and absorption rates only if the spontaneous emission rate,

$$W_{sp} = \frac{4\ w^3}{3c^3\hbar} |\mu_{ab}|^2, \qquad \text{(II-27)}$$

for the transition $b \to a$ is much slower than stimulated emission or absorption. The stimulated emission and absorption rates are found by monitoring $|\langle a|T(t)|b\rangle|^2$ over time intervals that are long compared to $\tau = 2\pi/w$.

The requirement that T(t) be unitary for all times t provides the basis for a convenient measurement of the error accumulation, in time, of T(t) resulting from the use of (II-23) and (II-24), since terminating the series (II-22) is the only approximation made in the context of the semi-classical treatment used here. The unitarity requirement can also be used to check for large computer programming blunders.

For a model two level system, T(t) can be written as a 2x2 matrix, and the requirement that T be unitary becomes

$$T\ T^+ = I, \qquad \text{(II-28)}$$

where $^+$ denotes the Hermitian adjoint and I the identity matrix. Hence, Trace $(T\ T^+)$ = $Tr(T\ T^+)$ must equal two if

T is to be unitary, and the unitarity requirement for T(t) for an n-level system is

$$\mathrm{Tr}(T\,T^{+}) = n. \tag{II-29}$$

The physical interpretation of (II-29) can be found by noting that

$$\begin{aligned}\mathrm{Tr}(T\,T^{+}) &= \sum_{a\ 1}^{n}\ \sum_{b=1}^{n} (T_{ab})\ (T_{ba})^{+} \\ &= \sum_{a=1}^{n}\ \sum_{b=1}^{n} T_{ab}\ (T_{ab})^{*} \\ &= \sum_{a,b} \langle a|T(t)|b\rangle\langle a|T(t)|b\rangle^{*} \qquad \text{(II-30)} \\ &= n.\end{aligned}$$

If the system is initially in the state b = 1 at time $t_o = 0$, at some later time t the atom or molecule must be in some one of the n states or a state composed of the linear combination

$$|\psi(t)\rangle = \sum_{a=1}^{n} \langle a|T(t)|b=1\rangle|a\rangle.$$

Thus, the sum of the sum of the transition probabilities for the transitions

(b=1) → (a=1)

(b=1) → (a=2)

...

(b=1) → (a=n)

must equal unity, and

$$\sum_{a=1}^{n} |\langle a|T(t)|b\rangle|^2 = 1. \qquad \text{(II-31)}$$

Hence, for any initial state b at $t_o = 0$, the manifold of transitions

$$b \to (a=1),\ b \to (a=2),\ \ldots\ b \to (a=n)$$

must satisfy Equation (II-31) at all later times, and Equation (II-30) follows.

An additional monitoring of calculational accuracy can be obtained by using T(t) to find the single photon absorption rates in multi-level systems. By comparing these rates with those predicted by the Rabi formula (13),

$$|a_{10}(t)|^2 = \frac{V_{01}^2}{\hbar^2(w_o-w)^2+V_{01}^2} \sin^2(t/2(w_o-w)^2 + (V_{01}/\hbar)^2)^{1/2}), \qquad \text{(II-32)}$$

large errors in the computer program used to calculate $|\langle a|T(t)|b\rangle|^2$ can be detected and eliminated, even though Equation (II-29) may be satisfied to a high degree of accuracy.

In practice, $U(\tau)$ is first calculated using the iterative process based on the series (II-22) and either Equation (II-23) or (II-24). $U(\tau)$ is then transformed into the Schroedinger representation and $T(\tau)$ generated. A convenient time unit

$$t' = 2^m \tau, \qquad \text{(II-33)}$$

with m an integer, is chosen and T(t') is generated by the process

$$T(2\tau) = (T(\tau))^2$$

$$T(4\tau) = (T(2\tau))^2$$

$$\cdots$$

$$T(2^m \tau) = (T(2^{m-1}\tau))^2.$$

$T(2^m \tau)$ is then multiplied out in $2^m\tau$ time units and the transition under consideration is monitored each $2^m\tau$ time increment through a computer printout of $|\langle a|T(t)|b\rangle|^2$, where

$$T(2\cdot 2^m \tau) = T(2^m\tau)\ T(2^m\tau)$$

$$T(3\cdot 2^m \tau) = T(2\cdot 2^m\tau)\ T(2^m\tau)$$

$$\cdots$$

$$T(q\cdot 2^m \tau) = T((q-1)\cdot 2^m\tau)\ T(2^m\tau).$$

In addition, $Tr(T\ T^+)$ is also printed out at each $2^m\tau$ increment as an indicator of calculational accuracy. From the printout of $|\langle a|T(t)|b\rangle|^2$, the period of the transition rate, assuming $|\langle a|T(t)|b\rangle|^2$ is proportional to $\sin^2(2\pi/\underline{\tau})t$, can be easily determined to within a factor of τ, where $\tau = 2\pi/w$ for the driving field and $\underline{\tau}$ is the period of the transition frequency. For single photon processes,

$$\underline{\tau} = 2\pi/\underline{w},$$

where

$$\underline{w} = \frac{1}{2}\left((w_o - w)^2 + (V_{ab}/\hbar)^2\right)^{1/2}$$

from Equation (II-32). For all double photon processes and most triple photon processes, except in multiple resonance systems, $|\langle a|T(t)|b\rangle|^2$ was found to fit a $\sin^2\Omega t$ function quite closely.

CHAPTER III

GENERAL REQUIREMENTS FOR MULTIPLE PHOTON ABSORPTION

As with the single photon absorption process, theoretical treatments of multiple photon absorption processes must allow for parity requirements in the absorbing molecule and the limitations imposed by spontaneous emission. In addition, a problem unique to multiple photon absorption is posed by the choice of driving field frequency, or frequencies.

The problem of parity is best illustrated by considering double photon absorption in the rotational spectrum of CD_3CN (microwave region). The mathematical model used for CD_3CN is a three level system. On the K=M=0 manifold, the energy levels for a typical symmetric-top molecule are given in Figure 1. For a symmetric-top molecule such as CD_3CN, the quantum number J determines the total angular momentum of the molecular system, while K determines the components of the total angular momentum along the unique axis of the molecule and M determines the component of the total angular momentum along the direction of any applied field. Since CD_3CN is a symmetric-top, it is subject to NH_3-type inversion. For ammonia, the frequency (14) of the "umbrella" inversion is approximately 2.4×10^{10} sec^{-1},

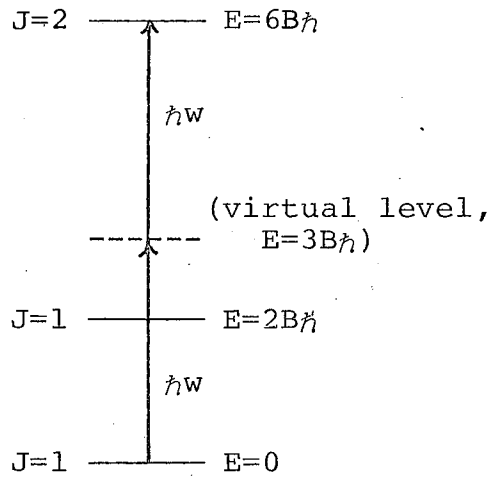

Figure 1. The K=M=O energy level manifold for a model three level symmetric-top molecule -- For CD_3CN, B is 4.937×10^{10} rad/sec. The vertical arrows indicate double photon absorption at w=3B.

while for CD_3CN the frequency is extremely slow (on the order of years) compared with transition rates for single, double, and triple photon absorption in the microwave region. If the parity of the vibrational and rotational parts of the total wavefunction is considered, each state specified by (J,K=M=O) can be shown (14) to be <u>two</u> states with (+) and (-) parity, respectively. For K=M=O, however, parity considerations for the nuclear spin wavefunctions for each (J,K=M=O) dictate that only (-) parity states can exist for J even, and (+) parity states for J odd. Double photon absorption in a symmetric-top molecule treated as a three level system on the K=M=O manifold is illustrated in Figure 2. The parity selection rules (+) $\leftrightarrow$ (+) and

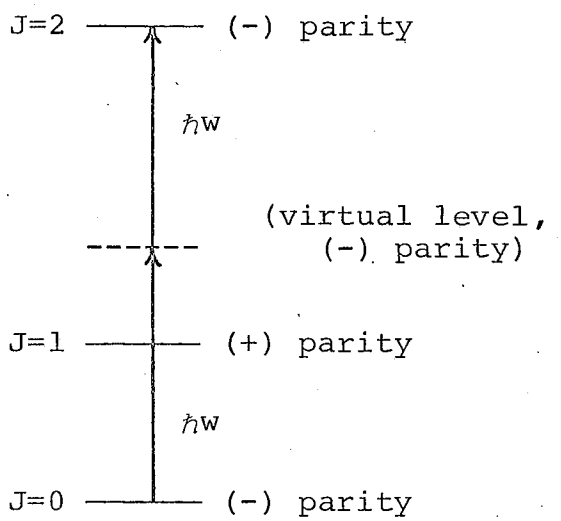

Figure 2. K=M=0 energy level manifold for a model three level symmetric-top molecule, with the parity of each J state indicated.

(-) ↔ (-) for double photon absorption of the type ΔJ=+2 are derived from the (+) ↔ (-) parity selection rule for the two single photon transitions involving the virtual level indicated by the dashed lines in Figures 1 and 2. The (+) ↔ (-) parity selection rule for single photon electric dipole transitions requires that the virtual level have (+) parity.

On the KM = ±1 manifold in CD_3CN, each angular momentum state specified by (J,K=±1, M=±1) is doubly degenerate, with one state having (+) parity and the other (-) parity. The two-fold degeneracy results both from the negligibly small inversion frequency of CD_3CN, and the parity behavior of the nuclear spin wavefunction when K≠0.

A schematic of the two photon absorption J=2↛↛3 for CD_3CN treated as a four level system is given in Figure 3. In order to guarantee that the transition occurs only on the KM = ±1 manifold, a Stark-modulation field must be used (10). For calculational purposes the symmetric-top molecule on the KM = ±1 manifold must be treated as a four level system to allow for the parity-induced degeneracy of each level and to prevent violations of the (+) ↔ (-) single photon parity selection rule.

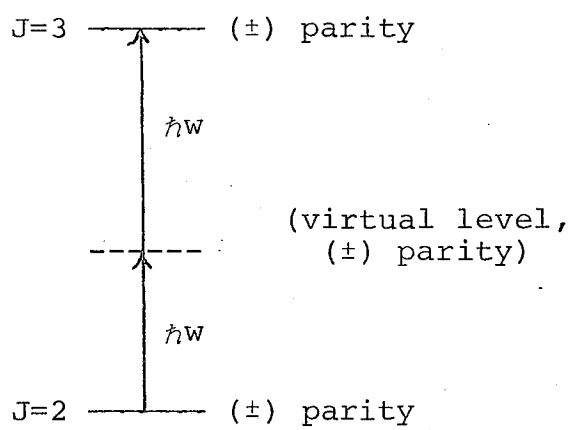

Figure 3. ΔJ=+1 double photon absorption on the KM=±1 manifold for a symmetric-top molecule treated as a four level system.

Triple photon absorption in CD_3CN is parity allowed for transitions of the type ΔJ=+1 and ΔJ=+3 on the K=M=0 manifold, as illustrated in Figure 4. For ΔJ=+3 triple

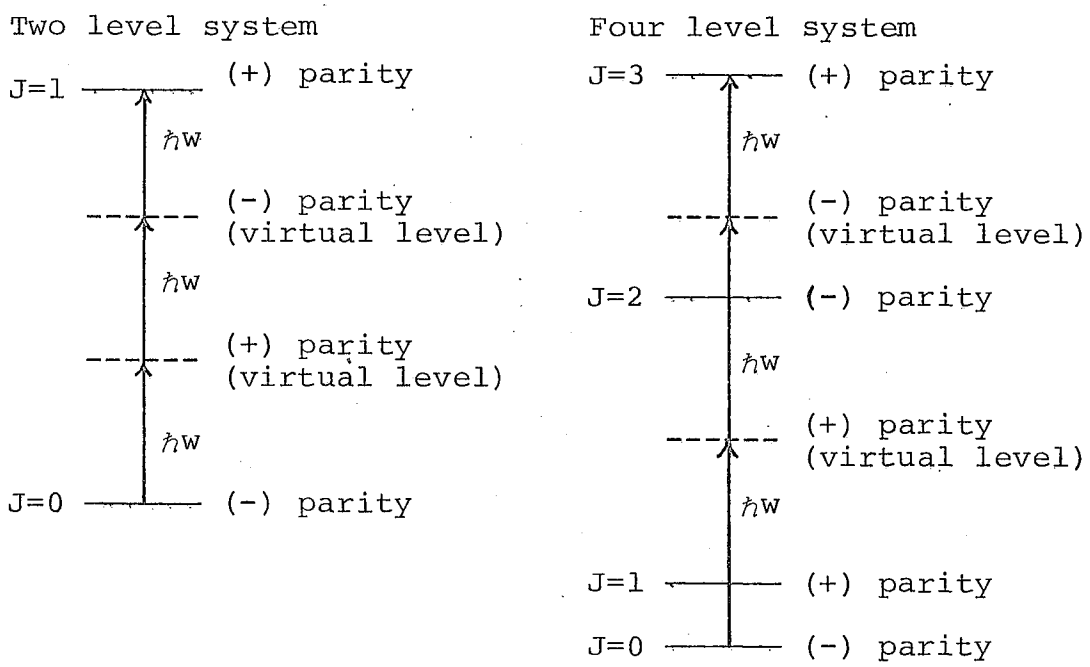

Figure 4. ΔJ=+1 and ΔJ=+3 triple photon absorption on the K=M=O energy level manifold for a symmetric-top molecule treated as a two level and a four level system respectively.

photon transitions in CD_3CN, the model used for the molecule is a four level system, while for triple photon transitions of the type ΔJ=+1 a two level system may be used to approximate CD_3CN. Similary, n-photon absorption, with n = 5,7,9, etc., is parity allowed for ΔJ=+1 transitions on the K=M=O manifold.

For model systems with equally spaced energy levels, such as a 3, 4, 5, or 6 level simple harmonic oscillator, it is no longer possible to discuss "pure" multiple photon transitions, since a multiple photon transition in such a

system will undoubtedly involve a multiple resonance phenomenon, or cascade of single photon transitions. The model used to represent a system with equally spaced levels was a system with three to six equally spaced levels, but without the relationship between successive dipole moment matrix elements typical of a simple harmonic oscillator. A single quantum, "step-ladder" cascade or quadruple resonance is illustrated schematically in Figure 5 for a five level system. In Figure 5 the sequence of transitions, if the system is initially in the ground state E_1, is $E_1 \rightarrow E_2 \rightarrow E_3 \rightarrow E_4 \rightarrow E_5$. If the system is in E_2 initially, the cascade sequence is $E_2 \rightarrow E_3 \rightarrow E_4 \rightarrow E_5$. The cascade sequence of single photon absorptions is expected to become less efficient in populating the uppermost level as the number of equally spaced levels is increased, due to the equal probabilities for stimulated emission and absorption at each step of the cascade "ladder" and due to level shifts.

The level shift phenomenon, discussed in several quantum optics papers (15-20), is particularly important to both the theories of multiple photon absorption and multiple resonances. Level shifts are observed only in the presence of resonant or nearly resonant radiation fields, so the phenomenon is a dynamic one which can be interpreted as a variation of the dc Stark effect. Qualitatively, each energy level of an atomic or molecular system in a radiation field "repels" all other energy levels, with the magnitude

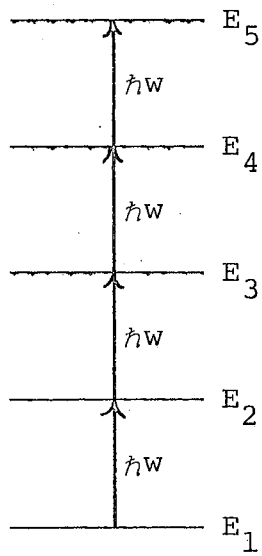

Figure 5. Quadruple resonance, or cascade absorption, for a model five level system with $\Delta E_{ij} = \hbar w$ for i, j = 1, 2, 3, 4, 5.

of the repulsion increasing with increasing driving field intensity. The result in the lab frame for a two level system is a resonance frequency shifted to a slightly higher frequency than would be observed in the limit of zero field intensity. The correct resonance frequency predicted by Bloch and Siegert (16) for a single photon transition in a two level system is

$$w = w_o + \frac{(\mu E)^2}{4\hbar^2 w} ,$$

where w_o is the resonance frequency in the limit of zero driving field intensity. The level shifts, exaggerated for clarity, are indicated schematically in Figure 6 for a two

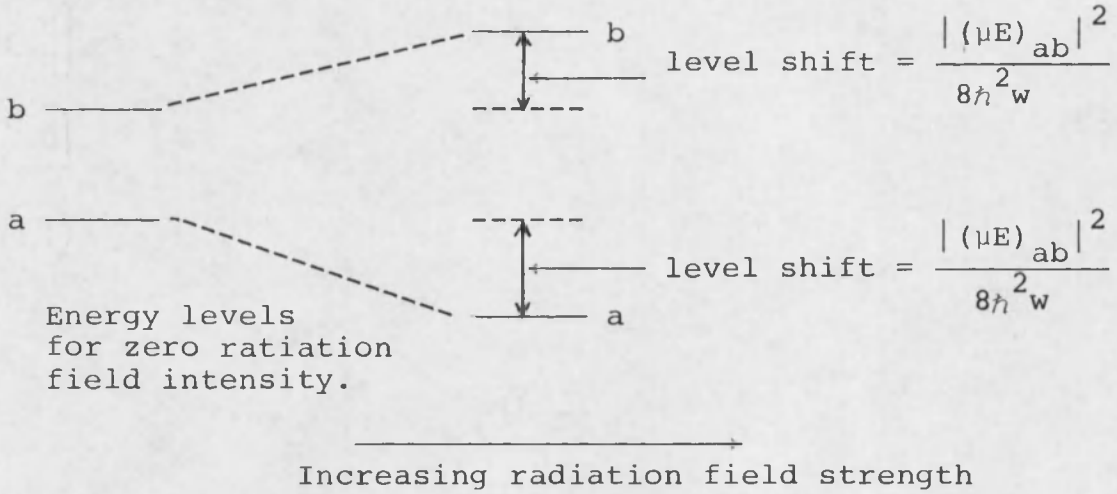

Figure 6. Level shifts, exaggerated for clarity, for two level system in a resonant, or nearly resonant, driving field (level shifts indicated are those predicted by Bloch and Siegert [16]).

level system. For traditional radiation sources of low intensity, the level shifts are small enough to ignore, but when high power lasers are used as radiation sources, the level shifts are expected to become fairly large (8). For two photon absorption of the type $\Delta J = +2$ for CD_3CN treated as a three level system on the K=M=O manifold, the level shifts predicted by Oka and Shimizu (10) are given by

$$\delta_c = \frac{|(\mu E)_z|_{12}^2}{\hbar^2} \quad \frac{(w-\Delta w)}{2(\Delta w)(w_o-\Delta w)}$$

for the J = 0 level, and

$$\delta_e = \frac{|(\mu E)_z|_{23}^2}{\hbar^2} \quad \frac{(w+\Delta w)}{2(\Delta w)(w_o+\Delta w)}$$

for the J = 2 level, where

$w = 3B$ = driving field frequency,

$w_o = 6B = \frac{E(J=2) - E(J=0)}{\hbar}$, and

$\Delta w = w - \frac{E(J=1)}{\hbar} = B$.

The correct resonance frequency is then $(1/2)(w_o+\delta_c-\delta_e)$. For a general three photon transition between adjacent levels a and b in a two level system, the net level shift predicted by Shirley (11) is

$$\delta = \frac{3|\langle|\mu_z E_z|b\rangle|^2}{8\hbar^2 w}$$

where w is the driving field frequency. If w_o specifies the resonance frequency of the a→b single photon transition in the limit of zero driving field intensity, the correct three photon resonance frequency is claimed by Shirley to be

$$w = \frac{(w_o+\delta)}{3} .$$

Although the double photon absorption processes considered in this paper will involve two photons of equal energy, it is possible to obtain double photon absorption if two photons of unequal energy are used (1, 10). If $\hbar w_o$ is the total energy needed to obtain a double photon transition, then the frequencies w_1 and w_2 of the two photons of unequal energy must be such that $w_o = w_1 + w_2$. Such double photon processes can be treated with relative ease using the theory developed in Chapter II only if

$$w_1 = m \cdot w_2 \quad \text{or} \quad w_2 = m \cdot w_1 \qquad \text{(III-1)}$$

with m = 2,3,4,..., since Equation (II-18) can be applied only if V(t) is periodic. If $w_1 = 2 \cdot w_2$ and

$$V(t) = \mu \cdot E_1 \sin(w_1 \cdot t) + \mu \cdot E_2 \sin(w_2 \cdot t), \qquad \text{(III-2)}$$

then $\tau_1 = 2\pi/w_1 = 2\pi/2 \cdot w_2 = \tau_2/2$, and $2\tau_1 = \tau_2$. Hence, if $\tau = \tau_2$,

$$V(t+\tau) = \mu \cdot E_1 \sin(w_1(t+2\tau_1)) + \mu \cdot E_2 \sin(w_2(t+\tau_2)) = V(t),$$

and the driving field is periodic with period $\tau = \tau_2 = 2\tau_1$. If two photons of unequal energy are used, care must be taken to avoid double resonances, such as would occur if the perturbation given by (III-2) were applied to CD_3CN with $w_1 = 2B$ and $w_2 = 4B$. If m in Equation (III-1) is not an integer, the iterative procedure for U(t) must be applied for all times t after the perturbation is switched on, resulting in excessively long computation times.

As mentioned previously, semiclassical radiation theory can be applied to multiple photon processes only if the spontaneous emission rate given by Equation (II-27) is much slower than the transition rate for the specific multiple photon process under consideration. For this reason, the microwave region, where spontaneous emission rates are quite low, is an excellent area for multiple photon absorption experiments. In order to observe two and three photon absorption in the infrared and visible regions

the driving field amplitude must be increased in proportion to the increase in driving field frequency in order to keep absorption rates higher than spontaneous emission rates.

Although semiclassical radiation theory cannot account for the form of the emitted fields in multiple photon processes, either spontaneous or stimulated, the problem is one of considerable interest and importance. Using a quantized radiation field, it should be possible to determine the frequency or frequencies of the radiation fields from spontaneous and stimulated emission in two and three photon absorption experiments, such as those outlined in Figures 1 and 4 for CD_3CN.

The basic framework for the computer programs used to calculate transition rates for multiple photon processes is given in Appendix A, along with a sample program. The model systems treated in this paper are:

1. A rigid rotor with three to six energy levels beginning with J=0, CD_3CN dipole moment matrix elements on the K=M=0 manifold, and CD_3CN energy level spacings. For convenient reference, the field strength, rotational constant, and dipole moment are those used by Oka and Shimizu (10) for CD_3CN, namely,

   E_z = 200 volt /cm (or approximately 53 watts/cm^2)

   B = 2π (7857.93 MHz)

   μ = 3.92 Debyes.

2. A system with three to six equally spaced energy levels, but with CD_3CN dipole moment matrix elements and an energy level separation equivalent to a microwave frequency (6B).

CHAPTER IV

DOUBLE AND TRIPLE PHOTON ABSORPTION IN THE CD_3CN MODEL SYSTEM

Using the CD_3CN model system described in the preceding section, double photon transition rates were calculated for $\Delta J=+2$ transitions in three, four, five, and six level systems. For the $\Delta J=+2$ transition in the three level system illustrated in Figure 1, the intermediate level (J=1) was shifted over the range from $0.50B\hbar$ to $5.50B\hbar$ in order to test the accuracy of the formula given by Oka and Shimizu (10) for double photon transitions in a model three level system in which the intermediate level between the initial and final states is by-passed. A transition of this type, using Oka and Shimizu's (10) notation, is illustrated in Figure 7. The level shift factors predicted by Oka and Shimizu were found to be of the correct magnitude but wrong sign. Oka and Shimizu's formula was also compared with T(t) calculations for other $\Delta J=+2$ transitions in CD_3CN model systems of four, five, and six levels, and in the equivalent three level systems. Triple photon absorption rates for $J=0 \rightarrow\rightarrow\rightarrow J=1$ and $J=0 \rightarrow\rightarrow\rightarrow J=3$ transitions in the CD_3CN model systems were also calculated. For the $J=0 \rightarrow\rightarrow\rightarrow J=1$ transition two, three, and four level systems were employed, while a four level system was used for the $\Delta J=+3$ transition. The

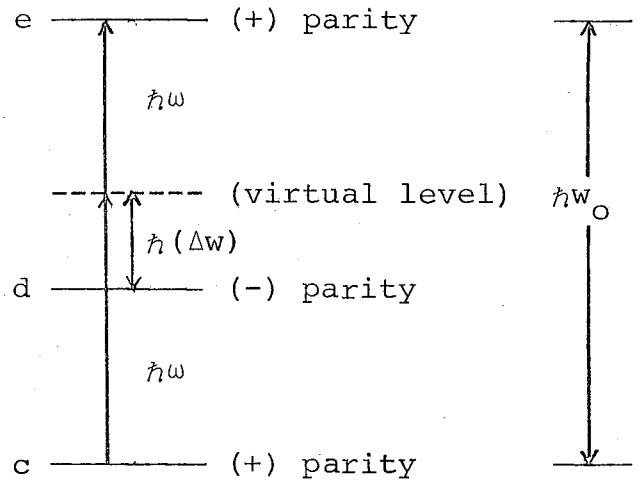

Figure 7. A model three level system for a symmetric-top molecule on the K=M=0 manifold using Oka and Shimizu's (10) notation

J=0 →→→ J=1 transition rates for a two level system compared fairly well with those predicted by Shirley (11), but for a four level system Shirley's formula is inadequate. Unless specified to the contrary, all of the T(t) calculations were performed to second order using Equation (II-24) with GRID= 1000, where δ of Chapter III is τ/GRID.

For the three level system depicted in Figure 7, the time-dependent transition probability predicted by Oka and Shimizu (10) for the double photon transition c → e is given by the relation

$$P_{c \to e} = \frac{A^2}{A^2+B^2} \sin^2 t(A^2+B^2)^{1/2} \qquad \text{(IV-1)}$$

where

$$A^2 = \frac{(\mu_z E_z)^2_{cd}(\mu_z E_z)^2_{de}}{16\hbar^4(\Delta w)^2}; \quad B^2 = ((1/2)(2w-w_o-\delta_c+\delta_e))^2$$

and

$$\delta_c = \frac{(\mu_z E_z)^2_{cd}}{\hbar^2 2(\Delta w)} \quad \frac{w - w}{w_o - w} \qquad \text{(IV-2)}$$

$$\delta_e = \frac{(\mu_z E_z)^2_{de}}{\hbar^2 2(\Delta w)} \quad \frac{w + w}{w_o + w} \; . \qquad \text{(IV-3)}$$

δ_e and δ_c are the level shifts for levels c and e, respectively. The level shift factor $(\delta_e - \delta_c)/2$ in Equation (IV-1) was found to have the incorrect sign. Hence, the correct resonance frequency is

$$w = \frac{w_o}{2} + \frac{\delta_e - \delta_c}{2} \qquad \text{(IV-4)}$$

and

$$P_{c \to e} = \frac{A^2}{A^2 + (B')^2} \sin^2 t(A^2 + (B')^2)^{1/2} \qquad \text{(IV-5)}$$

where

$$(B') = ((1/2)(2w - w_o + \delta_c - \delta_e))^2 .$$

The correct level shift factors that must be added to $w = w_o/2$ to yield complete resonance ($P(J=0 \nrightarrow 2) = 1$) are given in Table 1 for $J=0 \nrightarrow J=2$ double photon transitions in a three level CD_3CN model system in which the intermediate level was shifted over the range from $0.50B\hbar$ to $5.50B\hbar$. These level shift factors were verified using T(t) computer calculations in which the transition probability, given by $|\langle J=2|T(t)|J=0\rangle|^2$, was monitored in time at each 64τ time increment following t=0, with $\tau = 2\pi/w$. These calculations

Table 1. Level shift factors that must be added to $w=w_o/2$ for $J=0 \rightarrow\rightarrow J=2$ double photon transitions in a three level CD_3CN model system in which the intermediate level has been shifted over the range indicated (driving field frequency is $w=3B=1.481 \times 10^{11}$ rad/sec).

Intermediate level in B units	Level shift factor in rad/sec
0.50	1.55×10^6
1.00	1.30×10^6
1.50	1.01×10^6
1.80	8.93×10^5
2.00	5.93×10^5
2.10	4.66×10^5
2.30	1.16×10^5
2.50	-4.94×10^5
2.60	-1.02×10^6
2.80	-3.625×10^6
3.50	3.629×10^6
4.00	2.61×10^6
4.50	2.31×10^6
5.00	2.205×10^6
5.50	2.211×10^6

were performed both with, and without, the proper level shift factor included in the driving field frequency. The period of the transition frequency for each intermediate level location, measured in τ units and assuming a time-dependent transition probability $P(J=0\rightarrow\rightarrow1)$ proportional to a $\sin^2(\Omega t)$ function, was determined to within a factor of τ from the T(t) computer calculations and compared with that given by Equation (IV-5). Tables 2 and 3 indicate the results of this comparison in addition to the location of the first maximum in $P(J=0\rightarrow\rightarrow2)$ predicted by both the T(t) calculations and Equation (IV-5). The peak values for Equation (IV-5) were obtained from computer print-outs in 64τ time increments of the corrected Oka and Shimizu (10) formula. These print-outs were also used to determine the fit of T(t) to the corrected form of Equation (IV-1) both with, and without, the level shift factor given by (IV-4) included in the driving field frequency. The results of a typical fit are given in Table 4, and Tables 5 and 6 give the results of several such comparisons in terms of the magnitude of the maximum per cent error for probabilities between 0.1 and 1.0 over half a cycle of $P(J=0\rightarrow\rightarrow2)$.

It can be seen from Tables 2, 3, and particularly 5 and 6, that the corrected Oka formula inadequately describes the transition probability as the intermediate level approaches the energy of the photons of the driving field. Although a cascade from J=0 to J=2 is, strictly

Table 2. Comparison of transition periods computed from T(t) and Equation (IV-5) for J=0↠J=2 transitions in a three level CD_3CN model system in which the intermediate level has been shifted over the range indicated (driving field frequency is 3B in each case).

Intermediate level in B units	Transition period in τ units from corrected Oka	Transition period in τ units from T(t)	N=First maximum and location in τ units from T(t)	N=First maximum and location in τ units from corrected Oka
0.50	36789	36790	.850548 @ 144 (64τ)	.850640 @ 144 (64τ)
1.00	30733	30736	.927462 @ 120 (64τ)	.927541 @ 120 (64τ)
1.50	23618	23620	.973730 @ 92 (64τ)	.973799 @ 98 (64τ)
1.80	19047	19050	.989401 @ 75 (64τ)	.989536 @ 92 (64τ)
2.00	15923	15928	.995497 @ 63 (64τ)	.995911 @ 74 (64τ)
2.10	14345	14352	.997659 @ 56 (64τ)	.997962 @ 62 (64τ)
2.30	11168	11178	.999675 @ 44 (64τ)	.999742 @ 56 (64τ)
2.50	7975	7986	.996786 @ 31 (64τ)	.999235 @ 44 (64τ)
2.60	6376	6390	.994563 @ 25 (64τ)	.998039 @ 31 (64τ)
2.80	3181	3210	.984803 @ 12 (64τ)	.991041 @ 25 (64τ)
3.50	7829	7842	.962140 @ 30 (64τ)	.962762 @ 12 (64τ)
4.00	15360	15366	.926726 @ 60 (64τ)	.926769 @ 60 (64τ)
4.50	22426	22430	.877969 @ 88 (64τ)	.878009 @ 88 (64τ)
5.00	28822	28824	.815695 @ 113 (64τ)	.815786 @ 113 (64τ)
5.50	34269	34270	.738010 @ 133 (64τ)	.738118 @ 134 (64τ)

Table 3. Comparison of transition periods computed from T(t) and from Equation (IV-5) for J=0↔J=2 transitions in a three level CD_3CN model system in which the intermediate level has been shifted over the range indicated (driving field frequency includes the appropriate level shift factor).

Intermediate level in B units	Transition period in τ units from corrected Oka	Transition period in τ units from T(t)	N=First maximum and location in τ units from T(t)	N=First maximum and location in τ units from corrected Oka
0.50	39889	39990	.999870 @ 156 (64τ)	.999996 @ 156 (64τ)
1.00	31911	31912	.999892 @ 125 (64τ)	.999981 @ 125 (64τ)
1.50	23933	23938	.999870 @ 94 (64τ)	.999933 @ 93 (64τ)
1.80	19147	19150	.999932 @ 75 (64τ)	.999981 @ 75 (64τ)
2.00	15956	15960	.999680 @ 63 (64τ)	.999933 @ 62 (64τ)
2.10	14360	14366	.999703 @ 56 (64τ)	.999993 @ 56 (64τ)
2.30	11169	11178	.999756 @ 44 (64τ)	.999820 @ 44 (64τ)
2.50	7877	7990	.997478 @ 31 (64τ)	.999933 @ 31 (64τ)
2.60	6382	6396	.996448 @ 25 (64τ)	.999981 @ 25 (64τ)
2.80	3190	3222	.990023 @ 12 (64τ)	.996569 @ 12 (64τ)
3.50	7979	7990	.997572 @ 31 (64τ)	.999933 @ 31 (64τ)
4.00	15956	15960	.999718 @ 63 (64τ)	.999933 @ 62 (64τ)
4.50	23934	23938	.999901 @ 94 (64τ)	.999933 @ 93 (64τ)
5.00	31912	31912	.999892 @ 125 (64τ)	.999981 @ 125 (64τ)
5.50	39890	39990	.999908 @ 156 (64τ)	.999996 @ 156 (64τ)

Table 4. Typical fit of T(t) results to Equation (IV-5) -- The intermddiate level is at 1.90B$\hbar$ and no level shift factor has been included in the driving field frequency. $\underline{\tau}=64\cdot\tau$ and w=3B. The magnitude of the maximum per cent error for probabilities between 0.1 and 1.0 over half a cycle of $P_{c\to e}$ is 0.34%.

Time	T(t) result	Equation (IV-5) result	% Error
$15\underline{\tau}$	.113312	.113507	0.18%
$23\underline{\tau}$	.252567	.252766	0.08%
$35\underline{\tau}$	.515516	.515721	0.04%
$46\underline{\tau}$	.753296	.753741	0.06%
$55\underline{\tau}$	.902009	.902858	0.10%
$69\underline{\tau}$	.992728	.992922	0.02%
$81\underline{\tau}$	.911358	.911162	0.03%
$90\underline{\tau}$	.766578	.766249	0.05%
$102\underline{\tau}$	.508329	.507647	0.14%
$114\underline{\tau}$	.246217	.245761	0.19%
$122\underline{\tau}$	.108782	.108418	0.34%

Table 5. Comparison of Equation (IV-5) results with T(t) calculation results for two photon J=0↔J=2 transitions in CD_3CN model systems in terms of the per cent error as computed in Table 4 (no level shift factors included in the driving field frequency).

Intermediate level location in $B\hbar$ units	% Error
0.50	0.08%
1.60	0.31%
1.90	0.34%
2.00	0.41%
2.20	0.66%
2.40	0.96%
2.80	9.51%
4.00	0.59%
5.50	0.05%

Table 6. Comparison of Equation (IV-5) results with T(t) calculation results for two photon J=0↔J=2 transitions in CD_3CN model systems with level shift factors included in each driving field frequency as given in Table 1.

Intermediate level location in $B\hbar$ units	% Error
0.50	0.07%
1.60	0.22%
1.90	0.54%
2.00	0.40%
2.20	0.67%
2.40	1.72%
2.80	9.22%
4.00	0.41%
5.50	0.06%

speaking, only possible for the intermediate level at, or very near, the energy $E=3B\hbar$, the cascade effect becomes quite noticeable for the intermediate level located between 2.90B and 3.10B frequency units. This phenomenon will be discussed in greater detail in Chapter V.

The intrinsic accuracy of the T(t) calculations used in the above mentioned comparisons with Equation (IV-5) can be assessed by the requirement that T(t) be unitary for all times t. For a three level system, the unitary requirement is that $TR(T\ T^{+}) = 3$. The calculations used to generate T(t) were approximate, so it is expected that the unitarity of T(t) will decay for increasingly larger times $t > 0$. Table 7 displays the traces computed for various values of GRID for both first and second order T(t) calculations for the $J=0 \rightarrow\rightarrow J=2$ transition in a three level CD_3CN model system, with the intermediate level (J=1) in its "usual" location at $E/\hbar = 2B$. The traces in Table 7 were computed at the location of the first maximum in $P(J=0 \rightarrow\rightarrow 2)$, with time sampling increments of 64τ being employed. It is worthwhile to note that the calculations whose traces differ greatly from 3 also exhibit the greatest overshoot as $P(J=0 \rightarrow\rightarrow 2)$ approaches unity. Since the T(t) calculations tabulated in Tables 2 through 6 were performed to second order with GRID = 1000, the worst case trace can be taken to be on the order of 3.000 001 at the first peak in $P(J=0 \rightarrow\rightarrow 2)$.

Table 7. Calculational accuracy parameters for J=0↔J=2 two photon absorption in a three level CD_3CN model system ($\tau=2\pi/w=2\pi/3B$).

GRID	Peak value at time $t=62\cdot64\tau$	Trace at peak value	Period of transition frequency in τ units
First Order [Equation (II-23)]:			
100	1.064 746	3.2828	15 928
500	1.008 927	3.0541	15 928
1000	1.002 187	3.0269	15 928
Second Order [Equation (II-24)]:			
100	.995572	3.000 538	15 926
500	.995496	3.000 004 2	15 928
1000	.995497	3.000 000 3	15 928

Although the corrected Oka and Shimizu (10) formula was found to work quite well, with the one noted exception, for J=0↛J=2 transitions in the three level CD_3CN model system, it does not adequately predict the behavior of the same transition in CD_3CN rigid rotor model systems of four, five, or six levels, with $E(J) = J(J+1)B\hbar$ for J=0,1,2, ... The results of calculations for such systems are given in Table 8. It should be noted that the level shift factor is positive for the three level system, but negative for the four, five, and six level systems. This effect can most probably be attributed to the "repulsion" of the J=2 and J=3 energy levels under the influence of the driving field. In essence, the J=2 level is shifted by both the neighboring levels, J=1 and J=3, with the net effect being a negative level shift to lower apparent energy. As Table 8 indicates, the J=4 and J=5 levels have no observable effect on the net level shift factor. Once the four, five, and six level systems were properly level shifted, the transition periods were found to be identical to the transition period obtained for the three level system. When $|\langle J=2|T(t)|J=0\rangle|^2$ was fit to an $N\sin^2(\Omega t)$ function, with Ω being determined from the T(t) calculation with no level shift factor included in the driving field frequency and N a normalization factor equal to the first peak in $|\langle J=2|T(t)|J=0\rangle|^2$, the results, given in Table 9, were quite good. Hence, $|\langle J=2|T(t)|J=0\rangle|^2$ in a system of four or more levels still yields a $\sin^2(\Omega t)$

Table 8. Level shift parameters and results for $J=0 \leftrightarrow J=2$ transitions in CD_3CN model systems of three, four, five, and six energy levels, with $E(J)=J(J+1)B\hbar$ and GRID=1000.

Number of levels	Driving field frequency with level shift factor	N=First maximum in transition probability and location in τ units	Trace at peak location
3	3B	.995497 @ 63(64τ)	3.000 000 3
3	$3B + 5.931 \times 10^5$	.999680 @ 63(64τ)	3.000 000 3
4	3B	.983171 @ 62(64τ)	4.000 000 8
4	$3B - 1.19 \times 10^6$	.999652 @ 63(64τ)	4.000 000 8
5	$3B - 1.19 \times 10^6$	.999652 @ 63(64τ)	5.000 001 7
6	$3B - 1.19 \times 10^6$	.999652 @ 63(64τ)	6.005 652 3

Table 9. Comparisons of $|\langle J=2|T(t)|J=0\rangle|^2$ to an $N\sin^2(\Omega t)$ function for the $J=0 \leftrightarrow J=2$ transition in CD_3CN model systems of three, four, and five levels with Ω determined from T(t) calculations with GRID=1000.

Number of levels in system	Period in τ units from T(t) calculations	% Error
3	2(124(64τ) + 28τ)	0.80%
4	2(123(64τ) + 44τ)	0.10%
5	2(123(64τ) + 44τ)	0.10%

function, but with Ω being an even more complex function of level shift factors than in Equation (IV-5). T(t) calculations were also performed for the $J=0 \rightarrow\rightarrow J=2$ transition in CD_3CN model systems of four, five, and six levels, but with the system "scaled" by an order of magnitude in the sense that the parameters used in the calculations were $w=30B$, $E(J) = J(J+1)B\hbar$, and $E_z = 2000V/cm$, or equivalently, 5300 watts/cm^2. The results, given in Table 10, are identical to those given in the last three rows of Table 8, with the exceptions being that the level shift factor in Table 10 has been increased by an order of magnitude and $\tau = 2\pi/30B$.

Table 10. T(t) calculation results for the $J=0 \rightarrow\rightarrow J=2$ transitions in CD_3CN model systems with the systems "scaled" by an order of magnitude ($w=30B$, $E_z=2000V/cm$, and $\tau=2\pi/30B$).

Number of levels in system	N=First maximum in transition probability and location in τ units	Driving field frequency in rad/sec	Trace
4	.999652 @ 63(64τ)	$30B - 1.19 \times 10^7$	4.000 000 8
5	.999652 @ 63(64τ)	$30B - 1.19 \times 10^7$	5.000 001 7
6	.999652 @ 63(64τ)	$30B - 1.19 \times 10^7$	6.005 652 3

The corrected Oka and Shimizu (10) formula was also compared with the T(t) calculation results for the J=1↔J=3, J=2↔J=4, and J=3↔J=5 transitions in both multi-level CD_3CN model systems of four, five, or six levels with $E(J) = J(J+1)B\hbar$, and in the "equivalent" three level CD_3CN model systems. The corrected Oka formula was found to closely approximate the T(t) calculation results for the "equivalent" three level system, provided that the "systems" as "seen" by the corrected Oka formula were as given schematically in Figure 8 for the J=3↔J=5 transition. The remainder of the T(t) calculations, using systems of four, five, or six levels, employed the rigid rotor energy levels $E(J) = J(J+1)B\hbar$, with the lowest state being E(J) = 0. As Tables 12 and 13 show, the corrected Oka formula closely approximates the T(t) calculation results for the equivalent three level systems, even when the correct level shift factor is included in the driving field frequency. However, as Tables 11 and 13 indicate, the corrected Oka formula does not yield the correct transition parameters when a larger set of rigid rotor basis functions is employed. In particular, for both the J=2↔J=4 transition in a six level system, and the J=1↔J=3 transition in five and six level systems, there is negligible need for a level shift factor to achieve complete resonance. This result is most probably due to the level shift interaction between the levels directly involved in the transition and the nearest neighbor

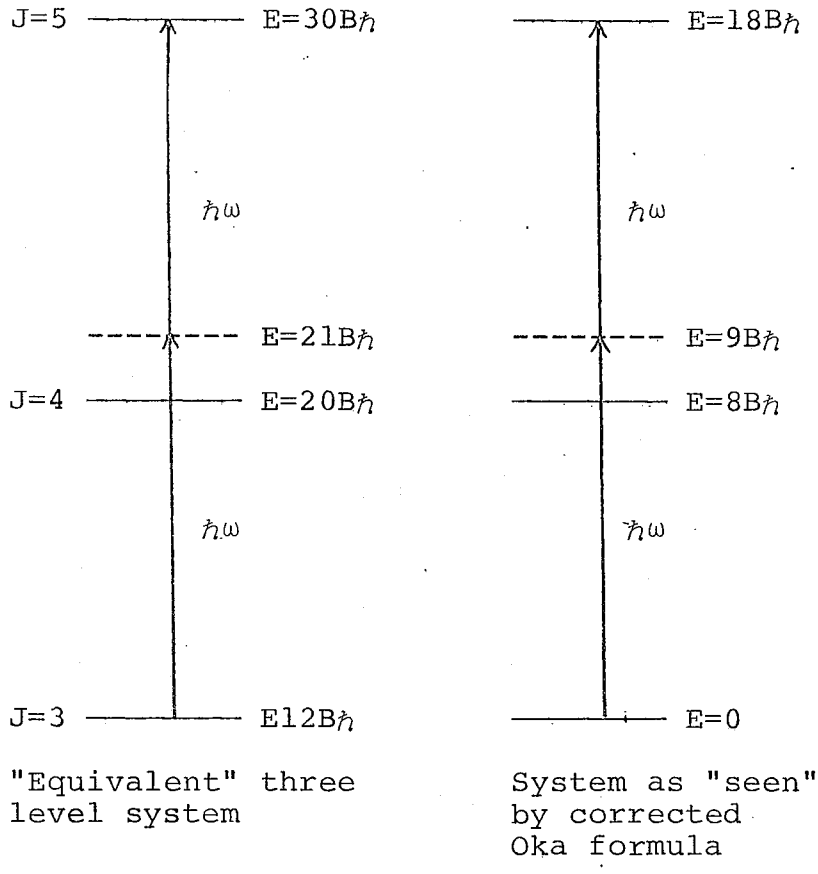

Figure 8. The "equivalent" three level system for T(t) calculations and the same system appropriate for use in the corrected Oka formula for the double photon transition J=3↠J=5.

Table 11. T(t) calculation results for J=2↔J=4 and J=1↔J=3 transitions in CD_3CN model systems with GRID=1000 and no level shift factors in the driving field frequency.

Transition	Number of levels	N=First maximum in transition probability and location in τ units	Trace
J=2↔4	5	.964220 @ 168(64τ)	4.999 999 4
J=2↔4	6	.999888 @ 169(64τ)	6.002 779 0
J=1↔3	4	.959722 @ 116(64τ)	3.999 999 9
J=1↔3	5	.999736 @ 119(64τ)	5.000 000 0
J=1↔3	6	.999736 @ 119(64τ)	6.003 838 3

Table 12. Comparison of T(t) calculation results to either an $N\sin^2(\Omega t)$ function or the corrected Oka formula result for the equivalent three level system for J=1↔J=3, J=2↔J=4, and J=3↔J=5 transitions in CD_3CN model systems -- All three level systems were constructed as indicated in Figure 8. If the source of Ω is a T(t) calculation, Ω has been determined to within a factor of $2\pi/\tau$, where τ is the period of the driving field frequency. Any level shift factors used were calculated from the corrected Oka formula for the equivalent three level system. For all T(t) calculations, GRID=1000.

Transition	Number of levels	Ω	Source of Ω	% Error
J=1↔3	5	8.152×10^6	T(t)	0.13%
J=1↔3	3	8.179×10^6	T(t)	0.08%
J=1↔3	3	8.182×10^6	Corr. Oka	0.44%
J=1↔3	3	8.154×10^6	Corr. Oka	0.56%[a]
J=2↔4	5	8.099×10^6	T(t)	0.20%
J=2↔4	3	7.972×10^6	T(t)	0.11%
J=2↔4	3	7.974×10^6	Corr. Oka	0.57%
J=2↔4	3	7.957×10^6	Corr. Oka	0.60%[a]
J=3↔5	6	8.021×10^6	T(t)	0.20%
J=3↔5	3	7.894×10^6	T(t)	0.08%
J=3↔5	3	7.896×10^6	Corr. Oka	0.44%
J=3↔5	3	7.885×10^6	Corr. Oka	0.41%[a]

[a]Level shift factor included in driving field.

Table 13. Comparison of T(t) calculation results with the corrected Oka formula results for the equivalent three level system for J=1↔J=3, J=2↔J=4, and J=3↔J=5 transitions in CD_3CN model systems with GRID=1000.

Transition	Number of levels in T(t) calculation	N=First maximum in transition probability and location in τ units	Period of transition frequency in units	
			T(t)	Corr. Oka
J=1↔3	5	.9997 @ 118(64→)	30284	--
J=1↔3	3	.9927 @ 119(64τ)	30184	30173
J=2↔4	5	.9642 @ 167(64τ)	42674	--
J=2↔4	3	.9956 @ 169(64τ)	43354	43341
J=3↔5	6	.9668 @ 215(64τ)	55396	--
J=3↔5	3	.9966 @ 218(64τ)	56292	56273

levels not directly involved in the transition, as indicated in Figure 9 for the J=2↔J=4 transition in a six level CD_3CN model system. Apparently, as Table 11 indicates for the J=1↔J=3 transition, only the nearest neighbor levels are responsible for the level shifts, at least to the degree of accuracy inherent in the T(t) calculations used in this paper. Although the level shift factors predicted by the corrected Oka formula do not apply for a transition in a multi-level system such as that given in Figure 4, as Table 12 indicates, the time-dependent transition probability is still very closely approximated by an $N\sin^2(\Omega t)$ function.

Triple photon absorption rates were calculated for J=0↔↔↔J=1 and J=0↔↔↔J=3 transitions in CD_3CN model systems. For the J=0↔↔↔J=1 transition in the two level systems indicated in Table 17 (p. 56), the T(t) calculation results were compared with those predicted by the formula given by Shirley (11),

$$P_{a\to b} = \frac{C^2}{C^2+D^2} \sin^2(t/2)\,(C^2+D^2)^{1/2}, \qquad \text{(IV-6)}$$

where

$$C^2 = \left(\frac{(\mu E)^3_{ab}}{\hbar^3 16w^2}\right)^2, \quad D^2 = \left(3w-w_o-(3/8)\,\frac{(\mu E)^2_{ab}}{\hbar^2 w}\right)^2,$$

and $E_b-E_a/\hbar = w_o$, with w the driving field frequency. The level shift factor that must be added to the driving field frequency is

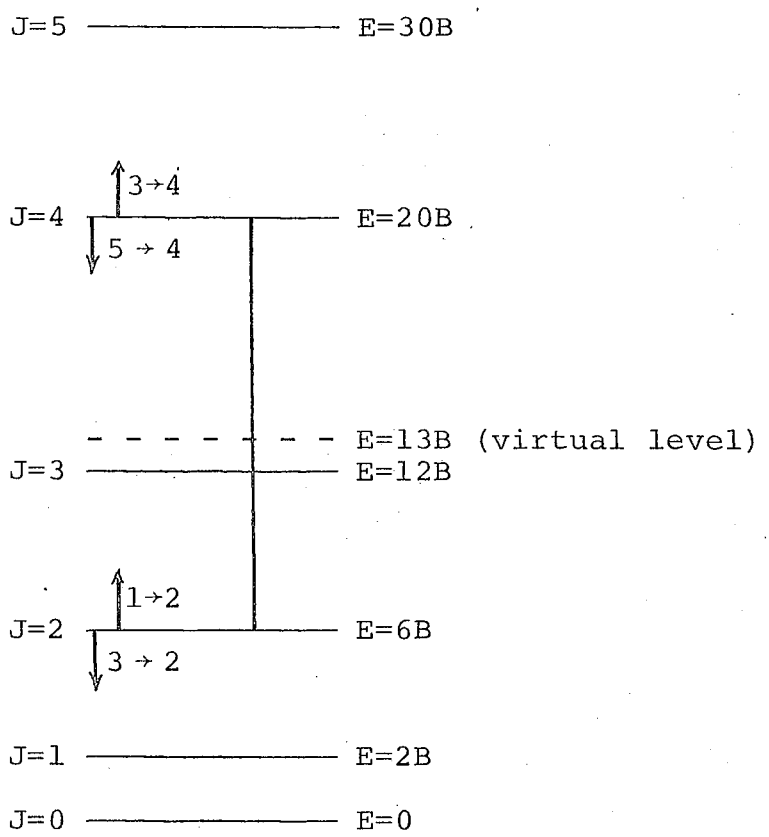

Figure 9. Schematic level shift interactions between the levels directly involved in a double photon transition and the nearest neighbor levels not directly involved in the transition -- The level shifts are indicated by 3→2, 1→2, 3→4, and 5→4, where 3→4 indicates the level shift in level 4 due to level 3.

$$\delta w = (1/8)\frac{(\mu E)^2_{ab}}{\hbar^2 w} \quad . \qquad \text{(IV-7)}$$

As Tables 14 and 15 indicate, Shirley's (11) formula inadequately describes the time-dependent transition probability and level shift factor, especially at higher driving field intensities. Table 16 lists a sample determination of the transition frequency for a triple photon transition. The effect of neighboring energy levels on the J=0↛↛J=1 transition was determined by performing T(t) calculations on three and four level CD_3CN model systems. The four level systems are those indicated in Table 17 with J=0,1,2,3. The three level system is identical to the system (w,E_z) but with J=0,1,2. As Tables 18 and 19 indicate, the level shifts and transition frequencies are quite different from those obtained for the same transitions in two level model systems. For driving fields of high intensity ($\geq$ 1000 watts), Table 18 shows that the time-dependent transition probability is no longer described with high accuracy by an $N\sin^2(\Omega t)$ function. A comparison of Tables 10 and 18 shows that the J=0↛↛J=1 transition "scales" with the same degree of accuracy as does the J=0↛↛J=2 double photon transition. A comparison of the results in Tables 14 and 15 with Table 18 reveals that while the Shirley formula does not yield accurate results for the J=0↛↛J=1 transition in four level systems, it does yield good order of magnitude estimates for

Table 14. T(t) calculation results for the J=0→→→J=1 transition in two level CD_3CN model systems -- The notation (w,E_z), $(10w,10E_z)$, and $(w,10E_z)$ is defined in Table 17. All three model systems used CD_3CN dipole moment matrix elements and GRID=4000. The per cent error column indicates the magnitude of the worst case per cent error when the T(t)-derived transition probability function was compared with an $N\sin^2(\Omega t)$ function for transition probabilities between 0.1 and 1.0 over half a cycle of $\sin(\Omega t)$, with Ω determined from the T(t) calculations as indicated in Table 16. In all cases the Trace at the first maximum in transition probability was on the order of 2.000 0007.

System	Level shift factor in rad/sec	N=First maximum in transition probability and location from T(t)	% Error
(w,E_z)	7.782×10^6	.999986 @ $95(2^{10}\tau)$	0.32%
(w,E_z)	7.781×10^6	.999536 @ $95(2^{10}\tau)$	--
$(10w,10E_z)$	7.782×10^7	.999986 @ $95(2^{10}\tau)$	--
$(10w,10E_z)$	7.781×10^7	.999536 @ $95(2^{10}\tau)$	--
$(w,10E_z)$	7.614×10^8	.999979 @ $103(2^{10}\tau)$	0.81%
(w,E_z)	7.784×10^6	.999000 @ $95(2^{10}\tau)$	0.57%
$(10w,10E_z)$	7.784×10^7	.999000 @ $95(2^{10}\tau)$	--
$(w,10E_z)$	7.784×10^8	.907763 @ $100(\tau)$	--

Table 15. Transition rates for the J=0→→→J=1 transition in two level CD_3CN model systems -- The T(t) and Shirley formula transition frequencies were calculated using their respective resonant level shift factors included in the driving field frequency. The T(t) transition frequencies were computed as indicated in Table 16.

System	Shirley formula transition frequency in rad/sec	T(t) transition frequency in rad/sec
(w,E_z)	8.464×10^4	8.461×10^4
$(w,10E_z)$	8.464×10^7	8.202×10^7
$(10w,10E_z)$	8.464×10^5	8.461×10^5

Table 16. Sample determination of the transition frequency for a triple photon transition -- τ is the period of the driving field frequency and the transition period in this case is $2(94 \cdot 2^{11} \cdot \tau + (1053/1054) \cdot 2^{11} \cdot \tau)$. The transition frequency is then just the driving field frequency in rad/sec divided by the transition period in τ units.

Time in $2^{11}\tau$ units	Transition probability
$94 \cdot 2^{11} \cdot \tau$	0.001053
$95 \cdot 2^{11} \cdot \tau$	0.000001
$96 \cdot 2^{11} \cdot \tau$	0.001135

Table 17. Explanation of the notation (w,E_z), $(w,10E_z)$, and $(10w,10E_z)$ used in Tables 14, 15, and 18 -- In all three cases CD_3CN dipole moment matrix elements were used.

System	Driving field frequency in B units	E_z in V/cm	Energy levels for J=0 and J=1
(w,E_z)	(2/3)B	200	$E(J)=J(J+1)B\hbar$
$(w,10E_z)$	(2/3)B	2000	$E(J)=J(J+1)B\hbar$
$(10w,10E_z)$	(2/3)B·10	2000	$E(J)=J(J+1)B\hbar 10$

Table 18. Comparison of T(t) calculation results for $J=0 \rightarrow\rightarrow\rightarrow J=1$ transitions in CD_3CN model systems of four levels with an $N\sin^2(\Omega t)$ function -- Ω has been determined from T(t) calculations as indicated in Table 15. $DE=9.489 \times 10^6$ rad/sec and all level shift factors are added to the driving field frequency.

System	Level shift factor in rad/sec	N=First maximum in transition probability and location from T(t)	Trace at first maximum	Ω from T(t) calculation	% Error
(w,E_z)	0.67DE	.999671 @ $123(2^{10}\tau)$	4.009 550[a]	6.536×10^4	0.16%
$(10w,10E_z)$	6.7DE	.999671 @ $123(2^{10}\tau)$	4.009 550[a]	6.536×10^5	3.2%
$(w,10E_z)$	66.0DE	.994494 @ $33(4\tau)$	4.000 116 9[b]	6.343×10^7	0.16%
$(w,10E_z)$	67.0DE	.915054 @ $33(4\tau)$	4.000 116 8[b]	6.449×10^7	2.88%

[a] GRID=1000.

[b] GRID=2000.

Table 19. T(t) calculation results for the J=0→→→J=1 transition in a three level (J=0,1,2) CD_3CN model system and a four level (J=0,1,2,3) CD_3CN model system (the level shift factor was 0.67DE and time sampling increments of $2^{10}\tau$ were employed in all cases).

	Three level system		Four level system	
GRID	N=First maximum in transition probability and location	Trace at first maximum	N=First maximum in transition probability and location	Trace at first maximum
1000	.999639 @ 123($2^{10}\tau$)	3.004	.999671 @ 123($2^{10}\tau$)	4.0096
2000	.998739 @ 123($2^{10}\tau$)	3.0004	.998770 @ 123($2^{10}\tau$)	4.001
3000	.998655 @ 123($2^{10}\tau$)	3.0001	.998685 @ 123($2^{10}\tau$)	4.0003
6000	.998623 @ 123($2^{10}\tau$)	2.999 98	.998653 @ 123($2^{10}\tau$)	3.999 99

the transition frequencies and level shift factors in the model systems denoted by (w,E_z), $(w,10E_z)$, and $(10w,10E_z)$. The results displayed in Table 19 indicate that to a very high degree of accuracy the J=3 level has negligible effect on both the net level shift factor and the transition rate for the J=0↛↛J=1 transition. Hence, as for double photon transitions, only the nearest neighbor levels produce a detectable level shift.

Results of the T(t) calculation of the transition rate for the J=0↛↛J=3 transition are given in Table 20. The four level system used for this transition is identical to the system denoted (W,E_z) and used in the J=0↛↛J=1 transition rate calculations, but with w=4B. In addition to comparing the triple photon transition probability to an $N\sin^2(\Omega t)$ function, attempts were made to fit the transition probability magnitude as a function of driving field frequency to the lineshape function

$$\mathcal{L}(w) = N = \frac{(\Delta w/2)^2}{(w-w_o)^2+(\Delta w/2)^2} , \qquad \text{(IV-8)}$$

for both the J=0↛↛J=1 transition in the four level system $(w,10E_z)$ and the J=0↛↛J=3 transition in the four level system (w,E_z). For the J=0↛↛J=3 transition, $\Delta w/2$ was computed using the relation

$$\frac{(\Delta w)^2}{2} = \frac{N}{1-N}(w-w_o)^2 , \qquad \text{(IV-9)}$$

Table 20. Comparison of T(t) calculation results for the $J=0 \rightarrow\rightarrow\rightarrow J=3$ transition in the CD_3CN model system of four levels with a $N\sin^2(\Omega t)$ function -- Ω has been determined from the T(t) calculations as indicated in Table 15, $DE=9.489 \times 10^6$ rad/sec, the time sampling increments were $2^{14}\tau$, all level shift factors were added to the driving field frequency, and GRID=1000.

Level shift factor in rad/sec	N=first maximum in transition probability and location in time	Trace at first maximum	Ω from T(t)	% Error
0.047DE	.991364 @ $100(2^{14}\tau)$	4.000 068 1	2.968×10^4	0.32%
0.046DE	.751819 @ $88(2^{14}\tau)$	4.000 058 6	3.406×10^4	0.91%

with w_o=4B + 0.0472DE. Table 21 displays some of the data points used to calculate $\Delta w/2$. The average value of $\Delta w/2$ was found to be 1.971 x 10^4 rad/sec. ± 3%, where ±3% indicates the worst case deviation from the average value over the frequency range w=4B + 0.040DE to w=4B + 0.052DE. For the J=0→→→J=1 transition Equation (IV-9) was again used, with w_o = (2/3)B + 65.7DE. The resulting average value of $\Delta w/2$ had worst case deviations of +17% and -27% over the range indicated in Table 22, which displays a few of the data points used. An attempt was made to secure a more accurate value of w_o for this transition by writing Equation (IV-9) as

$$\frac{N_2}{1-N_2}(w_2-w_o)^2 = (\Delta w/2)^2 = \frac{N_1}{1-N_1}(w_1-w_o)^2$$

and solving for w_o, with the data points (N_1,w_1) and (N_2,w_2) bracketing the apparent resonance frequency w_o such that $N_1 \cong N_2$. Six such pairs of points were used to calculate six different values of w_o, with the average value corresponding to w_o = (2/3)B + 115.8DE. Hence, the transition probability function for the J=0→→→J=1 transition in a four level system cannot be described in the time domain by a $\sin^2(\Omega t)$ function or in the frequency by a Lorentzian, if high intensity driving fields are used.

It should be noted that both the two level and four level systems denoted (w,E_z) scale quite accurately, as

Table 21. Some of the T(t)-derived data points used to fit the transition probability amplitude for the J=0→→→J=3 transition to Equation (IV-8) (w_o = 4B + 0.0472DE, w = 4B, and DE = 9.489 x 10^6 rad/sec).

Driving field frequency	N=first maximum in transition probability	w/2
w + 0.040DE	.0769	1.972 x 10^4
w + 0.045DE	.472732	1.977 x 10^4
w + 0.0465DE	.899766	1.990 x 10^4
w + 0.047DE	.991354	2.032 x 10^4
w + 0.0475DE	.978462	1.919 x 10^4
w + 0.052DE	.157150	1.967 x 10^4

Table 22. Some of the T(t)-derived data points used to fit the transition probability amplitude for the J=0→→→J=1 transition to Equation (IV-8) (w_o = (2/3)B + 65.7DE, w = (2/3)B, and DE = 9.489 x 10^6 rad/sec).

Driving field frequency	N=first maximum in transition probability	w/2
w + 58DE	.326311	5.085 x 10^7
w + 65.6DE	.999616	4.842 x 10^7
w + 65.7DE	.999845	--
w + 65.8DE	.999063	3.099 x 10^7
w + 74DE	.158690	3.421 x 10^7

Tables 14 and 18 indicate for the systems denoted (w,E_z) and $(10w,10E_z)$. In essence, scaling the driving field frequency, energy levels, and field amplitude by a factor of ten produces a factor of ten increase in the transition frequency. The fact that the system (w,E_z) scales exactly to $(10W,10E_z)$ indicates that the computer program used to generate the T(t) results works properly, as can be verified by examination of Equation (II-24).

CHAPTER V

MULTIPLE RESONANCE ABSORPTION IN CD_3CN MODEL SYSTEMS

It was noted in the previous chapter that the corrected Oka and Shimizu (10) formula began to break down as the intermediate (J=1) level approached 3B in the three level CD_3CN model system with E(J=0)=0, E(J=2)=6B$\hbar$ and a driving field frequency of w=3B. In this chapter T(t) calculation results will be given for various intermediate level locations over the range 2.90B$\hbar$ to 3.10B$\hbar$. In addition, T(t) results will be given for a model system of five equally spaced levels with energy spacings of 6B$\hbar$, a driving field frequency w=6B, and CD_3CN dipole moment matrix elements.

Table 23 displays the T(t) calculation results using the three level system and compares the single photon transition probabilities with a $N\sin^2(\Omega t)$ function. Table 23 also displays the results predicted by the Rabi formula for the J=0→J=1 single photon transition. The transition probabilities for E(J=1)≠3B$\hbar$ for the double photon J=0→→J=2 transition appeared to be modulated by the transition probability function for the J=0→J=1 single photon transition, as Figure 10 indicates for the intermediate level located at 2.95B$\hbar$. Strictly speaking, for E(J=1)=3B$\hbar$ the J=0→→J=2 transition

Table 23. T(t) calculation results for three level CD_3CN model systems with the intermediate level, J=1, shifted over the range indicated -- In all cases w=3B. The per cent error column indicates the magnitude of the per cent error when the T(t) calculated transition probability for the J=0→J=1 single photon transition is compared with a $N\sin^2(\Omega t)$ function for transition probabilities between 0.1 and N over half a cycle of the transition frequency. Ω is obtained from the T(t) calculation.

Intermediate level in B units	N=first maximum in probability for J=0→J=1 transition from T(t)	N=first maximum predicted by Rabi formula for J=0→J=1 transition	N for the J=1→J=2 transition from T(t)	N for the J=1→J=2 transition from Rabi formula	% Error for J=0→J=1 transition	N=first maximum in transition probability for J=0→→J=2 transition	Period of transition frequency for J=0→J=1 in τ units	
							Rabi formula	T(t)
2.90	0.0757 @ 14τ	0.0092 @ 5τ	.0564 @ 14τ	.0074 @ 5τ	--	.9900 @ 419τ	56	20
2.95	0.2135 @ 24τ	0.036 @ 10τ	.1644 @ 24τ	.029 @ 10τ	4.56%	.9824 @ 237τ	94	39
2.975	0.3973 @ 32τ	0.130 @ 19τ	.3111 @ 32τ	.107 @ 19τ	0.31%	.9724 @ 130τ	130	75
3.00	0.5554 @ 39τ	1.0 @ 51τ	.4443 @ 39τ	1.0 @ 58τ	1.66%	.9876 @ 77τ	154	207
3.025	0.3888 @ 32τ	0.130 @ 19τ	.3178 @ 32τ	.107 @ 19τ	2.69%	.9707 @ 130τ	130	75
3.05	0.2054 @ 24τ	0.036 @ 10τ	.1708 @ 24τ	.029 @ 10τ	--	.9784 @ 237τ	95	39
3.10	0.0705 @ 14τ	0.0092 @ 5τ	.0605 @ 14τ	.0074 @ 5τ	--	.9824 @ 419τ	56	20

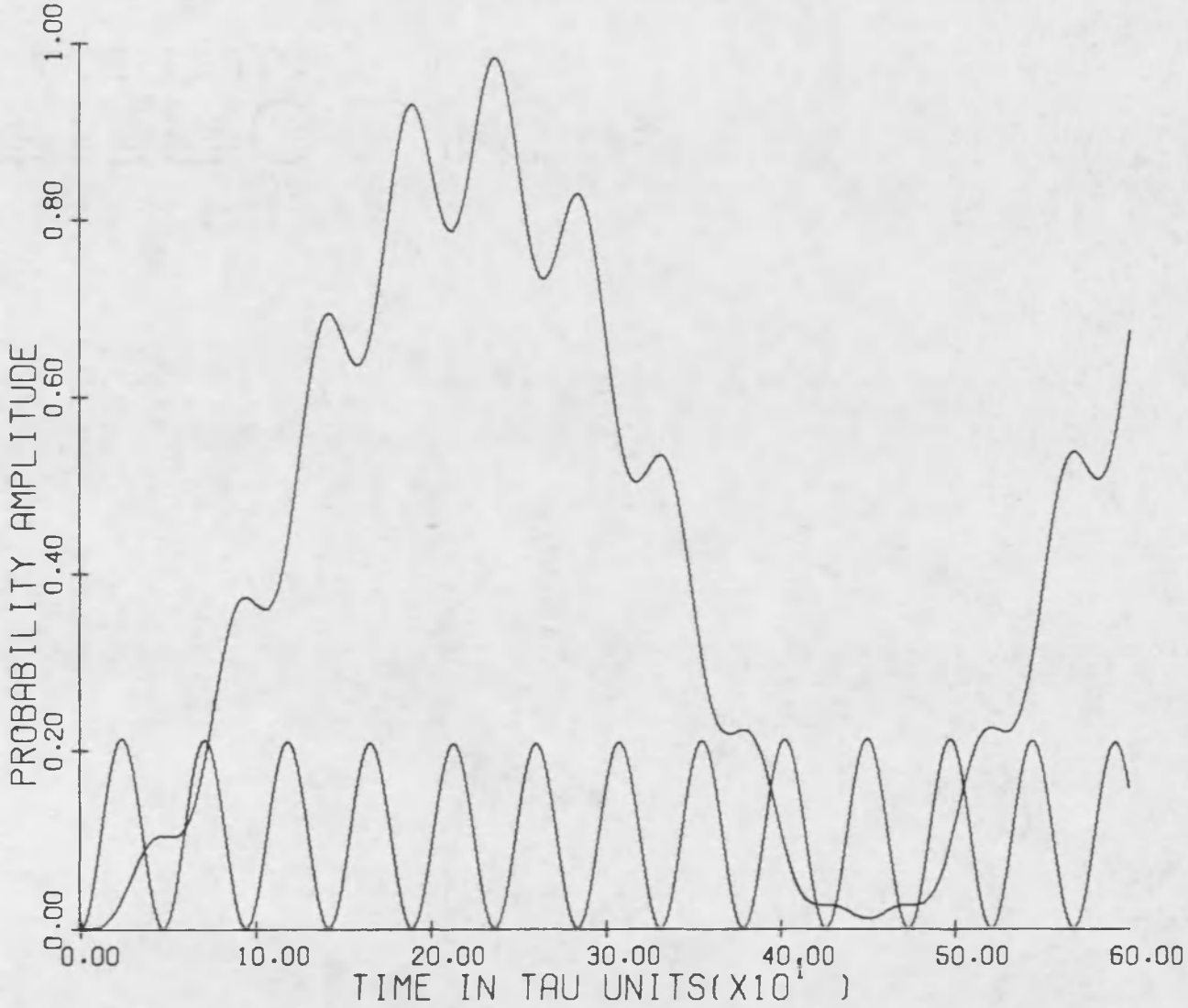

Figure 10. Time-dependent transition probabilities for the J=0→J=1 single photon transition and J=0↔J=2 double photon transition (maximum amplitude curve) for the intermediate level located at $2.95B\hbar$.

cannot be described either as a pure double photon transition or a pure double resonance transition, but rather as a mixture or hybrid of both. For the intermediate level located exactly at $3B\hbar$, the J=0→J=2 double resonance transition probability could not be accurately fit to a $N\sin^2(\Omega t)$ function, even though it does not appear to be modulated by the J=0→J=1 single photon transition probability function, as Figure 11 indicates. The increase in the J=0→J=1 single photon transition rate, indicated in Table 23 by a comparison of the Rabi formula predictions with the T(t) results, can be attributed in part to the small energy separation between the existing intermediate level and the required virtual level, combined with a "bootstrap" effect provided by the double photon resonance. A similar increase in the J=1→J=2 single photon transition rate was also observed. In essence, these increases appear to indicate that both the double and single photon transition rates benefit from a nearly resonant intermediate level and that the single and double photon processes act cooperatively. This double quantum resonance enhancement has also been predicted by Roberts and Fortson (7) in the context of high-resolution double quantum laser spectroscopy.

Table 24 and Figures 12 and 13 display the T(t) results for the model system of five equally spaced levels illustrated in Figure 5 and the manifold of transitions $E_1 \rightarrow E_1$, $E_1 \rightarrow E_2$, $E_1 \rightarrow E_3$, $E_1 \rightarrow E_4$, and $E_1 \rightarrow E_5$ for which the sum of

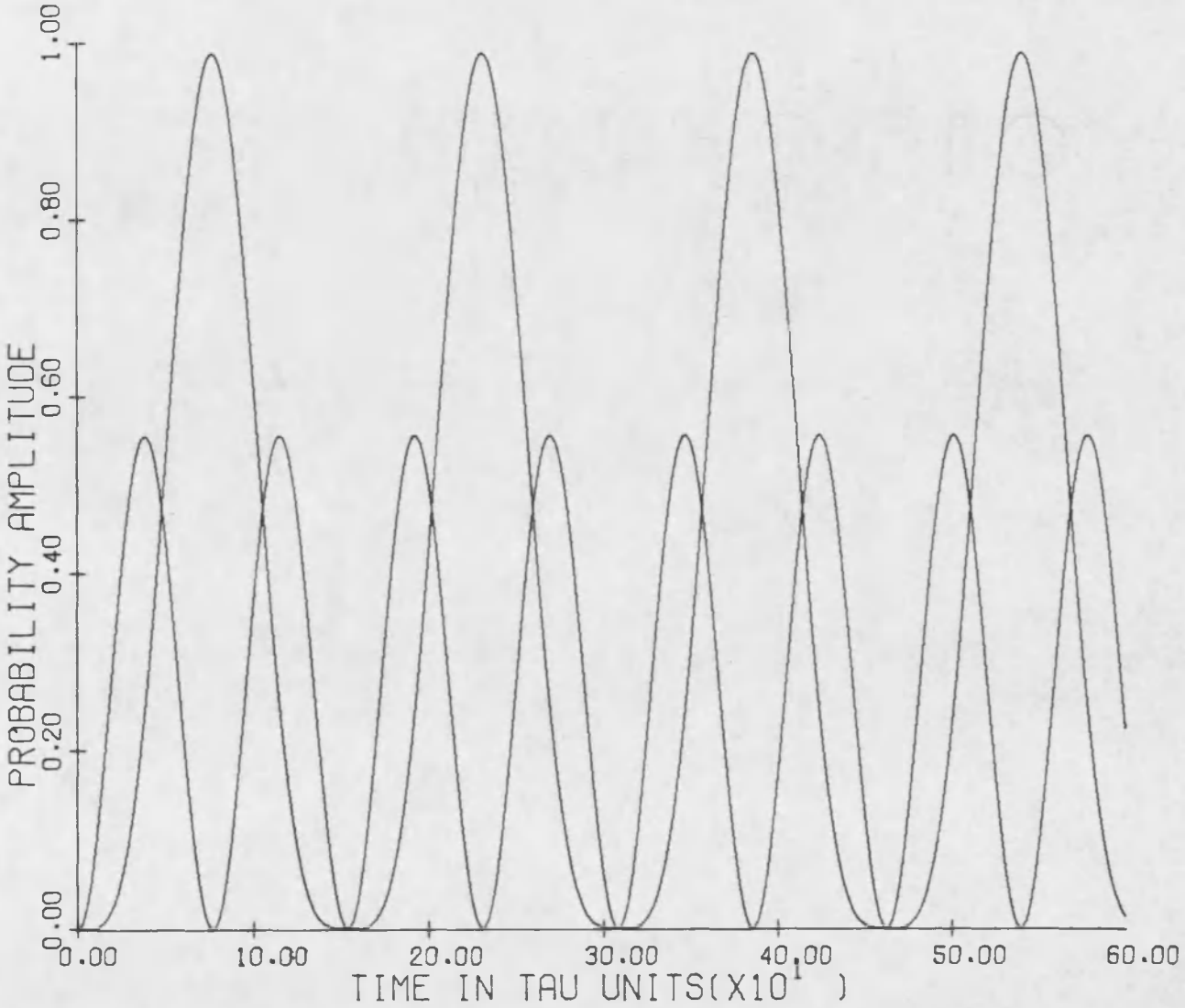

Figure 11. Time-dependent transition probabilities for the J=0→J=1 single photon transition and J=0↠J=2 double photon transition (maximum amplitude curve) for the intermediate level located at $3.00B\hbar$.

Table 24. Locations and values of first maxima in transition probability for the manifold of transitions $E_1 \rightarrow E_2$, $E_1 \rightarrow E_3$, $E_1 \rightarrow E_4$, and $E_1 \rightarrow E_5$ for the model system of five equally spaced energy levels with CD_3CN dipole moment matrix elements.

Transition	First maximum	Transition probability at 242τ	First minimum
$E_1 \rightarrow E_2$	.570748 @ 79τ	.095579	.000034 @ 170τ
$E_1 \rightarrow E_3$	.472522 @ 127τ	.007394	.000001 @ 227τ
$E_1 \rightarrow E_4$	.365092 @ 165τ	.000048	.000048 @ 242τ
$E_1 \rightarrow E_5$	.896003 @ 242τ	.896003	.000001 @ 362τ

For times $t \leq 1000$, Trace $\leq$ 5.000 000 4 and the sum of the transition probabilities for the manifold of transitions $E_1 \rightarrow E_1, E_2, E_3, E_4, E_5$ was within the limits .999 999 6 to 1.000 000 4.

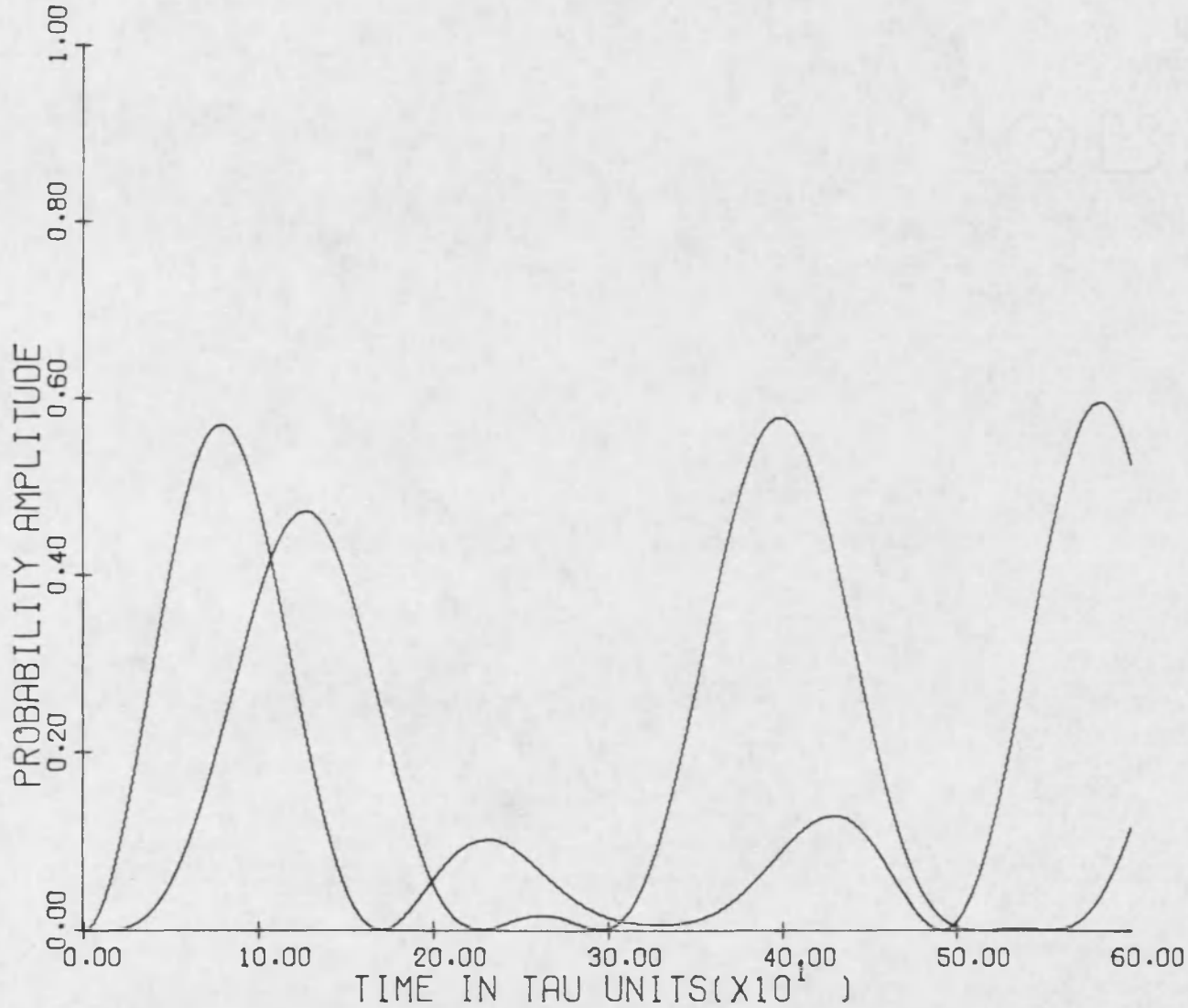

Figure 12. Time-dependent transition probabilities for the $E_1 \rightarrow E_2$ (curve with first maximum) and $E_1 \rightarrow E_3$ transitions in a model system with five equally spaced levels.

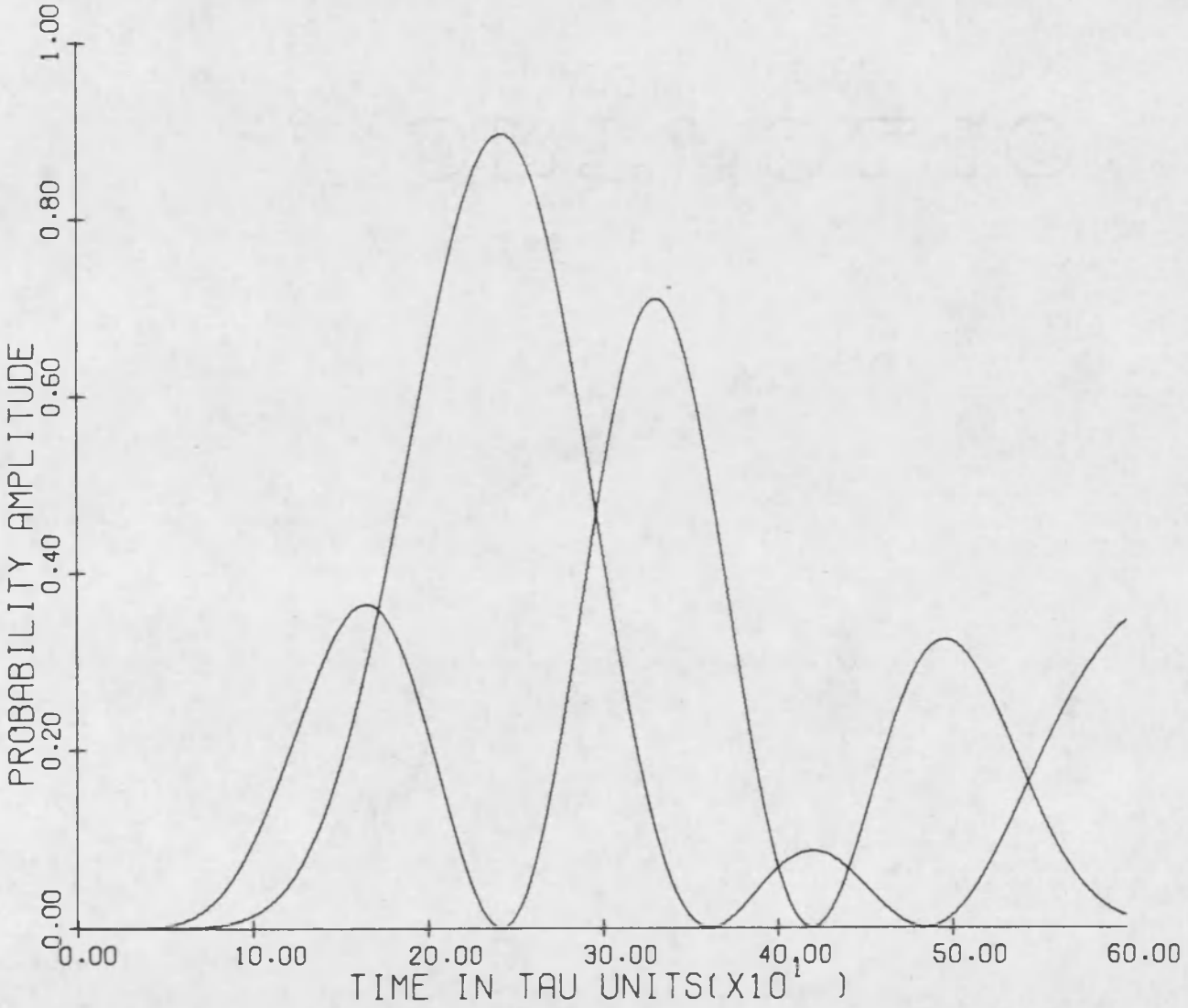

Figure 13. Time-dependent transition probabilities for the $E_1 \rightarrow E_4$ (curve with first maximum) and $E_1 \rightarrow E_5$ transitions in a model system with five equally spaced levels.

the transition probabilities at any specified time t must equal unity. Table 23 shows that the first maximum in the transition probability for the $E_1 \rightarrow E_5$ transition results from a step-wise build up in probability that appears to "flow" through first the $E_1 \rightarrow E_2$ transition, then through the $E_1 \rightarrow E_3$ transition, then the $E_1 \rightarrow E_4$ transition, and finally crests at the $E_1 \rightarrow E_5$ transition, which then rapidly drops to zero. It should be noted that the $E_1 \rightarrow E_5$ transition probability drops to the first minimum in a time significantly shorter than that required to reach the first maximum. Calculations for analogous model systems of four and six equally spaced levels with $\Delta E = 6B\hbar$ were also performed, yielding results quite similar to those for the five level system. In the model four level system the first maximum in the transition probability for the $E_1 \rightarrow E_4$ transition was .9401, while in the model six level system the first maximum in the transition probability for the $E_1 \rightarrow E_6$ transition was .8551. Hence, as the number of equally spaced levels is increased, the first maximum in the transition probability for the highest order multiple photon transition decreases in magnitude.

CHAPTER VI

DISCUSSION OF RESULTS AND CONCLUSIONS

Although the time evolution operator technique employed in this paper does not yield analytic expressions for time-dependent transition probabilities for two or three photon absorption, it is nevertheless a highly accurate method for testing the validity of previously derived theoretical expressions. In addition, it can provide high accuracy estimates of transition frequencies in systems that can only be treated approximately by the cumbersome technique of time-dependent perturbation theory, provided the driving field is periodic in times short compared with the transition frequency so that the relation $T(n\tau) = (T(\tau))^n$ can be applied effectively.

It was demonstrated in Chapter IV that for double photon transitions of the general form illustrated in Figure 1, the expression given by Oka and Shimizu (10) for the time-dependent transition probability is incorrect due to a sign error in the expression for the net level shift factor. Although the corrected Oka formula was found to fit the time evolution operator calculations for three level systems to a very high degree of accuracy, it should be noted that even the corrected Oka formula applies rigorously only to a pure

three level system. For double photon transitions in systems of four or more levels, the level shift factors were found to interact in a complex manner. In particular, if the three levels directly involved in the transition, such as those in Figure 1, are sandwiched between lower and higher energy levels, the net level shift factor is very small, as the results of Table 11 indicate. In addition, only the nearest neighbor energy levels above and below the three levels directly involved in the transition appear to have a significant effect on the net level shift factor, as Table 11 again indicates. The net level shift factor need not be positive, as Table 8 indicates for the $J=0 \rightarrow\rightarrow J=2$ double photon transition in CD_3CN rigid rotor model systems of four, five, and six levels. Table 8 also gives further evidence in support of the assertion that only the nearest neighbor levels above or below the three levels directly involved in the double photon transition appear to have a significant effect on the net level shift factor. In essence, only a five level system is needed to completely describe a two photon transition of the type illustrated in Figure 9, provided the additional two levels are located such that one is above level e and one is below level c, and assuming that the initial state for the double photon transition is not the ground state. If the initial state is the ground state, only a four level system is required, as Table 8 indicates. The results in Table 8 imply that the

double photon resonance frequency measured by Oka and Shimizu (10) for the J=0↠J=2 transition is slightly less than $(1/2)w_o = 3B$, while Table 11 indicates that for double photon transitions of the type J=1↠J=3, J=2↠J=4, etc. the net level shift factor would be small and difficult to observe experimentally.

Although the corrected Oka formula is accurate only in a three level model system, the results of Chapter IV indicate that even if a model system of more than three levels is used, the corrected Oka formula will yield estimates of the transition frequency that are accurate to better than two per cent, provided the system "seen" by the corrected Oka formula is treated as a three level system such as indicated in Figure 2. Additionally, the above discussion indicates that unless the initial state for the double photon transition is the ground state, the net level shift contribution to the resonance frequency will be negligible. The primary source of error in using the corrected Oka formula for systems of four or more levels appears to be the net level shift factor, which in turn determines the exact double photon resonance frequency.

The results given in Chapter IV for triple photon transitions indicate that the relation given by Shirley (11) for the triple photon transition probability function in model two level systems is inadequate for high intensity driving fields. For moderate driving field intensities, Shirley's

relation is reasonably accurate in predicting the correct transition frequency and net level shift factor. Shirley's relation cannot be expected to work accurately for triple photon transitions between two adjacent levels when the model model system contains more than the two levels directly involved in the transition. As in the two photon case, the level shift interactions become complex when model systems having an excess of energy levels are used. For the $J=0 \rightarrow\rightarrow\rightarrow J=1$ transition in the four level CD_3CN model systems denoted (w,E_z), $(w,10E_z)$, and $(10w,10E_z)$ the net level shift factors are somewhat smaller than in the equivalent two level systems, indicating that the effect of the J=2 level is to "push" the J=1 level down slightly. In addition, the J=3 level appears to have a negligible effect on the $J=0 \rightarrow\rightarrow\rightarrow J=1$ transition, as Table 19 indicates. Hence, as in the two photon case, only the nearest neighbor levels produce detectable level shifts for any given level. It should also be noted that for high intensity driving fields in systems having an excess of levels, the transition probability function is no longer accurately described by a $\sin^2(\Omega t)$ function, as the results for the four level CD_3CN model system denoted $(w,10E_z)$ indicate. In addition, the lineshape function for this model system could not be fit to a Lorentzian, although the lineshape function for the $J=0 \rightarrow\rightarrow\rightarrow J=3$ transition in a four level system could be fit to a Lorentzian. Hence, Shirley's formula yields at best order

of magnitude estimates for triple photon transition frequencies and net level shift factors.

The results in both Chapters IV and V indicate that the corrected Oka and Shimizu (10) formula loses accuracy as the energy separation between either the initial and intermediate levels or the intermediate and final levels approaches the energy of the photons of the driving field. If this energy separation equals $\hbar w$, the transition corresponds to a double resonance or cascade absorption. The results in Tables 2, 3, 4, and 5 indicate that for the energy separation different from $\hbar w$ by as much as ±10%, the corrected Oka formula begins to noticeably decay in accuracy. For an energy separation different from $\hbar w$ by ±3.33% or less, corresponding to shifting the intermediate level over the range $2.90B\hbar$ to $3.10B\hbar$, the single photon transition probabilities become detectably higher than those predicted by the Rabi formula, as Table 23 indicates. By considering the product

$$\frac{\text{(Peak Probability Amplitude from T(t))}}{\text{(Peak Probability Amplitude from Rabi formula}} \cdot$$

$$\frac{\text{(Transition frequency from T(t))}}{\text{(Transition frequency from Rabi formula)}}$$

an estimate can be obtained of the increased single photon transition rate in the double photon system with an energy separation within ±3.33% or less of $\hbar w$. Using the results from Table 23, this product can be seen to be between 1.5

and 2.9 for an energy separation in the range $2.90B\hbar$ to $3.10B\hbar$, but where the energy separation does not exactly equal $\hbar w$. As stated in Chapter V, these increases appear to indicate that both the single and double photon transition rates benefit from a nearly resonant intermediate level, and that the single and double photon processes act co-operatively. If such a system were observed experimentally, it would be difficult to distinguish between single and double photon absorption, were it not for the much narrower absorption bandwidth associated with double photon transitions.

For multiple resonance transitions in systems of four or more equally spaced levels, the most important feature of both the single and multiple photon transition probability functions is the total lack of periodicity. The results given in Chapter V for the model system of five equally spaced levels indicate that after the first peak in the transition probability for the four photon, quadruple resonance transition there is no discernible pattern to any one transition, including single photon transitions. For double photon transitions in three level CD_3CN model systems with equally spaced levels, such as the model CD_3CN system with the intermediate (J=1) level shifted over the range $2.90B\hbar$ to $3.10B\hbar$, both the single and double photon transition probability functions were periodic in time, even

though the double photon probability function could not be fit to a $N\sin^2(\Omega t)$ function.

Although double photon transitions have been observed in the microwave region (10) and in the visible region using pico-second, mode-locked laser pulses and dye absorbers with inherently large absorption bandwidths, it is useful to consider the power and frequency stability of a radiation source if double or triple photon absorption is to be detected experimentally. In the microwave, double resonance techniques (10) have proved quite useful in the detection of inherently weak double photon transitions. Double resonance detection of two or three photon absorption processes places two strong restrictions on the absorbing atomic or molecular system. The first is that the two or three quantum transition frequency or rate cannot be drastically smaller than the Rabi formula transition frequency for the single photon transition used to monitor the two or three quantum absorption. This monitoring radiation is generally weak compared with the intensity of the radiation field used to "pump" the multiple photon absorption. Secondly, the spontaneous emission rate out of the final state of the two or three quantum transition cannot exceed the multiple photon transition rate into the excited state. These two requirements limit the utility of double resonance techniques in the infrared and visible spectral regions, as Table 25 indicates. Table 25 lists the approximate

Table 25. Approximate transition frequencies for single, double, and triple photon transitions, plus the spontaneous emission rate, for various driving field frequencies and intensities for an atomic or molecular system with a transition dipole of one Debye -- Unless specified, the driving field intensity is approximately 120 watts/cm^{2}CW, equivalent to 1 statvolt/cm. For double photon transitions $\mu_{cd} \cong \mu_{de} \cong 1$ Debye. The frequencies $\nu \cong 2.8 \times 10^{13}$Hz and $\nu \cong 2.8 \times 10^{14}$Hz correspond to the frequencies of a CO_2 laser and a Nd:glass laser respectively.

								E_z = 10 statvolts/cm or 12kW power/cm^2			E_z = 100 statvolts/cm or 1.2Mwatts power/cm^2		
Driving field frequency	10^{10}Hz	10^{11}Ha	10^{12}Hz	2.8×10^{13}Hz	2.8×10^{14}Hz	5×10^{14}Hz	10^{15}Hz	2.8×10^{13}Hz	2.8×10^{14}Hz	5×10^{14}Hz	2.8×10^{13}Hz	2.8×10^{14}Hz	5×10^{14}
Spontaneous emission rate	$1.3(10^{-8})$	$1.3(10^{-5})$	$1.3(10^{-2})$	230	$2.3(10^5)$	$1.6(10^6)$	$1.3(10^7)$	230	$2.3(10^5)$	$1.6(10^6)$	230	$2.3(10^5)$	$1.6(10^6)$
Single photon transition frequency	$5(10^8)$	$5(10^8)$	$5(10^8)$	$5(19^8)$	$5(10^8)$	$5(10^8)$	$5(10^8)$	$5(10^9)$	$5(10^9)$	$5(10^9)$	$5(10^{10})$	$5(10^{10})$	$5(10^{10})$
Double photon transition frequency	$4(10^6)$	$4(10^5)$	$4(10^4)$	1400	140	80	40	$1.4(10^5)$	$1.4(10^4)$	8000	$1.4(10^7)$	$1.4(10^6)$	$8(10^5)$
Triple photon transition frequency	8000	80	8	10^{-3}	10^{-5}	$3.2(10^{-6})$	$8(10^{-7})$	1	10^{-2}	$3.2(10^{-3})$	10^3	10	3.2

transition frequencies for single, double, and triple photon transitions, plus the spontaneous emission rate, for various driving field frequencies and intensities for an atomic or molecular system with a transition dipole of one Debye. The double photon transition is assumed to be of the type given in Figure 1, with $\mu_{cd} = \mu_{de} = 1$ Debye. The double and triple photon transitions are assumed to be completely resonant, including level shift factors, with Equation (IV-5) used for the double photon transition and Shirley's (11) relation for the triple photon transition. In using (IV-5), Δw was taken to be the same as the driving field frequency. The Rabi formula was used for the single photon transition.

An alternate technique for both the detection and application of multiple quantum transitions is that of pumping a double or triple photon transition in conjunction with monitoring the resultant fluorescence from the excited state. The only serious limitation of this techique is the absorption bandwidth of double photon, and especially triple photon, processes. An examination of Equations (IV-5) and (IV-6) reveals that for double and triple photon processes the absorption linewidth has a HWHM equal to the transition frequency of the completely resonant (including level shift factors) system. Hence, the transition frequencies listed in Table 25 for double and triple photon absorption indicate the natural absorption linewidth in the absence of pressure and Doppler broadening. Table 25 indicates that for cw

laser sources, the double photon natural linewidths are too narrow for state-of-the-art frequency stabilized laser oscillators with frequency stabilities on the order of one part in 10^8. Tunable, frequency stabilized, cw lasers can be successfully used, however, as indicated by the atomic beam technique of Pritchard, Apt, and Ducas (3) which utilized a laser frequency scanning rate of 400 MHz/sec. For triple photon absorption the bandwidths in the infrared and visible are simply too small. If pulsed lasers with peak field amplitudes approaching 100 statvolts/cm (equivalent to about 1.2 Mwatts peak power) are used, the double photon absorption linewidths are on the order of 1-10 MHz. For triple photon absorption, the absorption bandwidths remain too small even at 1.2 Mwatts, except perhaps in the infrared. This technique for double photon absorption has recently been applied to atomic laser spectroscopy with considerable success. By using oppositely directed beams from a pulsed dye laser, Bloembergen and co-workers (4, 5) have been able to pump two quantum transitions while avoiding the problem of Doppler broadening in the double photon resonance line. The dye laser was tuned with an intracavity etalon, while the fluorescence from the excited state was monitored. The ultimate frequency sensitivity of such a technique is limited by the frequency stability of the laser (on the order of 20 MHz) and the natural linewidth of the excited state.

In summary, the results of the time evolution operator calculations given in this paper have been useful in several areas of the theory of multiple photon absorption. Oka and Shimizu's (10) formula has been corrected, with the corrected formula yielding results in excellent agreement with those from the time evolution operator calculations for model three level systems. The corrected Oka formula, as expected, is inadequate as the intermediate level, labeled d by Oka, approaches a location exactly in between the initial and final states of the double photon transition. For the intermediate level located such that $|E_d - E_c|$ was within 3.33% or less of $\hbar w$, the energy of the photons of the radiation field, the single photon transition probability was significantly higher than predicted by the Rabi formula. In essence, both the corrected Oka formula for double photon absorption and the Rabi formula for single photon absorption yield inaccurate predictions under these conditions. The corrected Oka formula was also found to be inadequate in model systems having additional neighboring energy levels adjacent to the three levels directly involved in the two photon transition. The inaccuracy of the corrected Oka formula in this case was primarily the result of the complex level shift interactions between the three levels directly involved in the transition and the nearest neighbor levels not directly involved in the transition. Hence, a three level model system is not sufficient to

completely determine the resonance frequency of a two photon transition as a function of the applied driving field. It should be noted, however, that if the three levels directly involved in the double photon transition are sandwiched between lower and higher energy levels, the net level shift factor is very small, assuming that the four transition dipoles appropriate to the five levels are essentially equal. For triple photon transitions between adjacent energy levels, the level shift contributions from neighboring levels not directly involved in the transition are even more important than in two photon transitions in determining the correct resonance frequency as a function of the applied field. For this reason Shirley's (11) formula cannot be applied with reasonable accuracy to calculations of triple photon transition frequencies or exact resonance frequencies. In addition, Shirley's formula is inadequate for high driving field intensities. Since the natural absorption linewidth of multiple photon transitions decreases with the number of simultaneously absorbed photons, the level shift interactions mentioned above cannot be ignored.

Finally, it can be concluded by examination of the single photon (Table 26), double photon (Tables 8 and 11), and triple photon (Table 19) results that in general only the nearest neighbor energy levels are responsible for the net level shift experienced by any given level for a general single, double, or triple photon transition.

Table 26. T(t) calculation results for the J=0→J=1 single photon transition in CD_3CN model systems of two, three, and four (J=0,1,2,3) levels -- For the system denoted $(w,E_z/10)$, E_z = (2/3)(1/10) statvolts/cm. For the three level system J=0,1, and 2.

System	Two levels N=first maximum in probability	Three levels N=first maximum in probability	Four levels N=first maximum in probability
(w,E_z)	.999393 @ 34τ	.999442 @ 34τ	.999442 @ 34τ
$(w,E_z)^a$	.999454 @ 34τ	.999476 @ 34τ	.999476 @ 34τ
$(w,E_z/10)$	.999998 @ 345τ	.999999 @ 345τ	.999999 @ 345τ
$(w,E_z/10)^a$	.999999 @ 345τ	.999999 @ 345τ	.999999 @ 345τ

[a]Denotes use of Bloch-Siegert shift in driving field frequency.

APPENDIX A

MECHANICS OF COMPUTER CALCULATIONS

The CD_3CN dipole moment matrix elements on the K=M=0 manifold are found from the relation (14)

$$\mu_z = \mu\phi(J,J')\ \phi_a\ (JK,J'K)\ \phi_z\ (JM,J'M) \qquad \text{(A-1)}$$

where μ is the total dipole moment of the molecule (3.92 Debyes), and for $J \rightarrow J' = J+1$ transitions,

$$\phi(J,J') = \frac{1}{4(J+1)((2J+1)(2J+3))^{1/2}}$$

$$\phi_a = 2((J+1)^2-K^2)^{1/2} = 2(J+1)$$

$$\phi_z = 2((J+1)^2-M^2)^{1/2} = 2(J+1).$$

Hence,

$$\mu_z = \mu \frac{J+1}{((2J+1)(2J+3))^{1/2}}, \qquad \text{(A-2)}$$

for J' = J+1 and K=M=0. For $J \rightarrow J' = J-1$,

$$\phi(J,J') = \frac{1}{4J(4J^2-1)^{1/2}}$$

$$\phi_a = 2(J^2-K^2)^{1/2} = 2J$$

$$\phi_z = 2(J^2-M^2)^{1/2} = 2J,$$

and

$$\mu_z = \mu \frac{J}{(4J^2-1)^{1/2}}. \qquad \text{(A-3)}$$

Thus,

$$(\mu_{01})_z = (\mu_{10})_z = \mu/(3)^{1/2}$$

$$(\mu_{21})_z = (\mu_{12})_z = 2\mu/(15)^{1/2}$$

$$(\mu_{32})_z = (\mu_{23})_z = 3\mu/(35)^{1/2} \ .$$

Since the zero index creates havoc with computers, the rotational energy levels are labeled one(J=0), two(J=1), ... , and the dipole moment matrix elements as

$$(\mu_{12})_z = (\mu_{21})_z = \mu/(3)^{1/2}$$

$$(\mu_{32})_z = (\mu_{23})_z = 2\mu/(15)^{1/2}$$

$$(\mu_{34})_z = (\mu_{43})_z = 3\mu/(35)^{1/2} \ .$$

Equation (II-8) can now be used to generate $V_I(t)$ for a completely general four level system. The Hamiltonian for a general four level system is

$$H_o = \begin{pmatrix} E_1 & 0 & 0 & 0 \\ 0 & E_2 & 0 & 0 \\ 0 & 0 & E_3 & 0 \\ 0 & 0 & 0 & E_4 \end{pmatrix} = \hbar \begin{pmatrix} I_1 & 0 & 0 & 0 \\ 0 & I_2 & 0 & 0 \\ 0 & 0 & I_3 & 0 \\ 0 & 0 & 0 & I_4 \end{pmatrix}$$

while the dipole moment matrix is

$$\begin{pmatrix} 0 & (\mu_{12})_z & 0 & 0 \\ (\mu_{21})_z & 0 & (\mu_{23})_z & 0 \\ 0 & (\mu_{32})_z & 0 & (\mu_{34})_z \\ 0 & 0 & (\mu_{43})_z & 0 \end{pmatrix}$$

Since $E_1/\hbar = I_1$, $E_2/\hbar = I_2$, etc.,

$$\exp(iH_o t/\hbar) = \begin{pmatrix} \exp(iI_1 t) & 0 & 0 & 0 \\ 0 & \exp(iI_2 t) & 0 & 0 \\ 0 & 0 & \exp(iI_3 t) & 0 \\ 0 & 0 & 0 & \exp(iI_4 T) \end{pmatrix}$$

and $V_I(t)$ for a general four level system interacting with a radiation field in the dipole approximation is

$$V_I(t) = -E_z \sin(wt) \; X$$

$$\begin{pmatrix} 0 & (\mu_{12})_z e^{(i(I_1-I_2)t)} & 0 & 0 \\ (\mu_{21})_z e^{(i(I_2-I_1)t)} & 0 & (\mu_{23})_z e^{(i(I_2-I_3)t)} & 0 \\ 0 & (\mu_{32})_z e^{(i(I_3-I_2)t)} & 0 & (\mu_{34})_z e^{(i(I_3-I_4)t)} \\ 0 & 0 & (\mu_{43})_z e^{(i(I_4-I_3)t)} & 0 \end{pmatrix} \tag{A-4}$$

If a second order calculation is to be performed using the iterative process based on Equation (II-24), $V_I'(t)$ and $(V_I(t))^2$ can be obtained from Equation (A-4).

In order to avoid direct manipulation of complex algebra by the computer, Equation (II-23) is written as

$$U(t+\delta) = (1+(\delta/i\hbar)V_I(t)U(t)$$

$$= (VR(t) + iVC(t))(UIR1(t) + iUIC1(t)), \tag{A-5}$$

where

$$VR(t) = Re\ (1 + (\delta/i\hbar)V_I(t)) \tag{A-6a}$$

$$VC(t) = Im\ (1 + (\delta/i\hbar)V_I(t)) \tag{A-6b}$$

$$UIR1 = Re\ (U(t)) \tag{A-6c}$$

$$UIC1 = Im\ (U(t)). \tag{A-6d}$$

It is important to note that VR is composed of the sum of an identity matrix and the real part of the matrix given by $(\delta/i\hbar)V_I(t)$. In a similar manner Equation (II-24) can be decomposed into real and imaginary parts using the same matrices as in Equations (A-6) for labeling convenience.

The iterative process for either the first or second order calculations now takes the form

$$\begin{aligned} U(n\delta) &= (VR((n-1)\delta) + (iVC((n-1)\delta))(UIR1((n-1)\delta) \\ &\quad + iUIC1((n-1)\delta)) \\ &= UIR1(n\delta) + iUIC1(n\delta) \end{aligned} \tag{A-7}$$

with a similar decomposition into real and imaginary parts being used for each δ time increment until $U(\tau)$ has been generated. Equation (II-10), with $t_o = 0$, can now be used to generate $T(\tau)$, where

$$T(\tau) = USR(\tau) + iUSC(\tau). \tag{A-8}$$

To generate $T(t'=2^m\tau)$, the matrix multiplication takes the form

$$T(2\tau) = (T(\tau))^2$$

$$= (USR(\tau) \cdot USR(\tau) - USC(\tau) \cdot USC(\tau))$$

$$+ i(USC(\tau) \cdot USR(\tau) + USR(\tau) \cdot USC(\tau)$$

$$= USR(2\tau) + iUSC(2\tau). \qquad \text{(A-9)}$$

In a similar manner, $T(t')$ is multiplied out in $2^m\tau$ time increments, with the transition probability at each time

$$t = q(2^m\tau), \quad q = 1,2,3,4, \ldots$$

given by

$$\langle a|T(t=q\cdot 2^m\tau)|b\rangle|^2 = (USR(a,b))^2 + (USC(a,b))^2.$$

```
      PROGRAM QOSC(INPUT,OUTPUT)
      DIMENSION UIC1(3,3),UIC2(3,3),UIR1(3,3),UIR2(3,3),VR(3,3)
      DIMENSION VC(3,3),C(3,3),S(3,3),USR(3,3),USC(3,3),USR1(3,3)
      DIMENSION USR2(3,3),USC1(3,3),USC2(3,3),U13(1000),U31(1000)
C CALCULATION FOR THREE LEVEL RIGID ROTOR MODEL SYSTEM
C F1=E(J=1)-E(J=0)=2B
C F2=E(J=2)-E(J=1)=4B
C F3=E(J=2)=6B
C F4=Z-COMPONENT OF(DIPOLE MOMENT)X(FIELD AMPLITUDE) FOR J=2,J=1
C F6=Z-COMPONENT OF(DIPOLE MOMENT)X(FIELD AMPLITUDE) FOR J=0,J=1
C W=DRIVING FIELD FREQUENCY
      IA=250
      N=3
      F1=9.874566064E+10
      F2=1.974913213E+11
      F3=2.962369819E+11
      F4=1.350464856E-18
      F6=1.50986548E-18
      W=1.481184910E+11
      DE=9.489461321E+6
      GRID=1000
      TAU=(2.*3.14159265)/W
      DT=TAU/GRID
C F5,F7,8,9,10,11,12 ARE NUMERICAL FACTORS RELATED TO THE MULTIPLICATIVE
C FACTORS IN EQUATION II-24
      F5=DT/(1.054592E-27)
      F7=(F5*DT)/2.
      F8=(F5**2)/2.
      F9=F4*F6
      F10=-(F6**2)*F8
      F12=-(F4**2)*F8
      F11=F10+F12
C SET ALL MATRIX ELEMENTS TO ZERO. VR,VC,UIR1,UIC1,USR,AND USC DEFINED IN
C APPENDIX A.
      DO 1 I=1,N
      DO 1 J=1,N
      UIC1(I,J)=0.
      UIC2(I,J)=0.
      UIR1(I,J)=0.
      UIR2(I,J)=0.
      VR(I,J)=0.
      VC(I,J)=0.
      C(I,J)=0.
      USR(I,J)=0.
      USC(I,J)=0.
      USR1(I,J)=0.
      USR2(I,J)=0.
      USC1(I,J)=0.
      USC2(I,J)=0.
    1 S(I,J)=0.
      DO 3 I=1,N
    3 UIR1(I,I)=1.
C START ITERATIVE PROCESS BASED ON EQUATION II-24.  ONLY NON-ZERO MATRIX
C ELEMENTS NEED BE COMPUTED.
      DO 20 L=1,1000
      T=0.+(L-1)*DT
      VC(2,3)=-F4*SIN(W*T)*COS(F2*T)*F5
```

```
      VC(3,2)=VC(2,3)
      VC(1,2)=-F6*SIN(W*T)*COS(F1*T)*F5
      VC(2,1)=VC(1,2)
      VR(2,3)=-F4*SIN(W*T)*SIN(F2*T)*F5
      VR(3,2)=-VR(2,3)
      VR(2,1)=F6*SIN(W*T)*SIN(F1*T)*F5
      VR(1,2)=-VR(2,1)
      VR(1,1)=1.+F10*((SIN(W*T))**2)
      VR(2,2)=1.+F11*((SIN(W*T))**2)
      VR(3,3)=1.+F12*((SIN(W*T))**2)
      VC(2,3)=VC(2,3)-W*COS(W*T)*COS(F2*T)*F4*F7+
     1F2*SIN(W*T)*SIN(F2*T)*F4*F7
      VC(3,2)=VC(2,3)
      VC(1,2)=VC(1,2)-W*COS(W*T)*COS(F1*T)*F6*F7+
     1F1*SIN(W*T)*SIN(F1*T)*F6*F7
      VC(2,1)=VC(1,2)
      VR(2,3)=VR(2,3)-W*COS(W*T)*SIN(F2*T)*F4*F7-
     1F2*SIN(W*T)*COS(F2*T)*F4*F7
      VR(3,2)=-VR(2,3)
      VR(2,1)=VR(2,1)+W*COS(W*T)*SIN(F1*T)*F6*F7+
     1F1*SIN(W*T)*COS(F1*T)*F6*F7
      VR(1,2)=-VR(2,1)
      VR(1,3)=-F8*F9*((SIN(W*T))**2)*COS(F3*T)
      VR(3,1)=VR(1,3)
      VC(1,3)=F8*F9*((SIN(W*T))**2)*SIN(F3*T)
      VC(3,1)=-VC(1,3)
C UIR2 AND UIC2 DEFINE U OPERATOR AT TIME L*DT
      DO 25 I=1,N
      DO 25 J=1,N
      DO 25 K=1,N
      UIR2(I,J)=UIR2(I,J)+((VR(I,K)*UIR1(K,J))-(VC(I,K)*UIC1(K,J)))
   25 UIC2(I,J)=UIC2(I,J)+((VR(I,K)*UIC1(K,J))+(VC(I,K)*UIR1(K,J)))
      DO 30 I=1,N
      DO 30 J=1,N
      UIC1(I,J)=UIC2(I,J)
      UIR1(I,J)=UIR2(I,J)
      UIR2(I,J)=0.
   30 UIC2(I,J)=0.
   20 CONTINUE
C TRANSFORM TO SCHROEDINGER REP. USR AND USC SPECIFY T OPERATOR.
      T=TAU
      C(1,1)=1.
      C(2,2)=COS(F1*T)
      C(3,3)=COS(F3*T)
      S(2,2)=SIN(F1*T)
      S(3,3)=SIN(F3*T)
      DO 35 I=1,N
      DO 35 J=1,N
      DO 35 K=1,N
      USR(I,J)=USR(I,J)+(C(I,K)*UIR1(K,J)+S(I,K)*UIC1(K,J))
   35 USC(I,J)=USC(I,J)+C(I,K)*UIC1(K,J)-S(I,K)*UIR1(K,J)
      DO 65 I=1,N
      DO 65 J=1,N
   65 PRINT 66,(I,J,USR(I,J),USC(I,J))
   66 FORMAT (I3,5X,I3,5X,F15.11,5X,F15.11)
      DO 40 I=1,N
      DO 40 J=1,N
```

```
      USR3(I,J)=USR(I,J)
      USC3(I,J)=USC(I,J)
      USR1(I,J)=USR(I,J)
   40 USC1(I,J)=USC(I,J)
C GENERATE TIME INCREMENT SPECIFIED BY II-33, 64*TAU IN THIS CASE.
      DO 45 L=1,6
      DO 50 I=1,N
      DO 50 J=1,N
      DO 50 K=1,N
      USR2(I,J)=USR2(I,J)+((USR(I,K)*USR1(K,J))-USC(I,K)*USC1(K,J))
   50 USC2(I,J)=USC2(I,J)+((USC(I,K)*USR1(K,J))+USR(I,K)*USC1(K,J))
      DO 55 I=1,N
      DO 55 J=1,N
      USR1(I,J)=USR2(I,J)
      USC1(I,J)=USC2(I,J)
      USR(I,J)=USR2(I,J)
      USC(I,J)=USC2(I,J)
      USR2(I,J)=0.
   55 USC2(I,J)=0.
C COMPUTE TRACE
      TR3=0.
      DO 75 I=1,N
      DO 75 J=1,N
   75 TR3=TR3+USR1(I,J)**2+USC1(I,J)**2
      PRINT 76,(TR3)
   76 FORMAT (40X,F12.7)
   45 CONTINUE
      DO 80 I=1,N
      DO 80 J=1,N
   80 PRINT 81,(I,J,USR1(I,J),USC1(I,J))
   81 FORMAT (I3,5X,I3,5X,F15.11,5X,F15.11)
C MULTIPLY T OPERATOR  OUT IN 64TAU TIME INCREMENTS.
      DO 92 L=1,IA
      DO 90 I=1,N
      DO 90 J=1,N
      DO 90 K=1,N
      USR2(I,J)=USR2(I,J)+((USR(I,K)*USR1(K,J))-USC(I,K)*USC1(K,J))
   90 USC2(I,J)=USC2(I,J)+((USC(I,K)*USR1(K,J))+USR(I,K)*USC1(K,J))
C COMPUTE TRANSITION PROBABILITY FOR J=0 TO J=2 TRANSITION
      U31(L)=USR2(3,1)**2+USC2(3,1)**2
      U13(L)=USR2(1,3)**2+USC2(1,3)**2
      DO 91 I=1,N
      DO 91 J=1,N
      USR1(I,J)=USR2(I,J)
      USC1(I,J)=USC2(I,J)
      USR2(I,J)=0.
   91 USC2(I,J)=0.
C COMPUTE TRACE AT L*64TAU
      TR3=0.
      DO 93 I=1,N
      DO 93 J=1,N
   93 TR3=TR3+USR1(I,J)**2+USC1(I,J)**2
      PRINT 94,(TR3)
   94 FORMAT (80X,F12.7)
      PRINT 95,(L,U13(L),U31(L))
   95 FORMAT (I5,5X,F12.6,5X,F12.6)
   92 CONTINUE
```

REFERENCES

1. Fruend, S. M., J. W. C. Johns, A. R. W. McKellar, and T. Oka, J. Chem. Phys. 59, 3445 (1970).

2. Kramer, P. B., S. R. Lundeen, B. O. Clark, and F. M. Pipkin, Phys. Rev. Lett. 32, 635 (1974).

3. Pritchard, D., J. Apt, and T. W. Ducas, Phys. Rev. Lett. 32, 641 (1974).

4. Levenson, M. D., and N. Bloembergen, Phys. Rev. Lett. 32, 645 (1974).

5. Bloembergen, N., M. D. Levenson, and M. M. Salour, Phys. Rev. Lett. 32, 867 (1974).

6. Goeppert-Mayer, M., Ann. Physik 9, 273 (1931).

7. Roberts, D. E., and E. N. Fortson, Phys. Rev. Lett. 31, 1539 (1973).

8. Bebb, H. B., and A. Gold, Phys. Rev. 143, 1 (1966).

9. Salzman, W. R., Phys. Rev. A 5, 789 (1972).

10. Oka, T., and T. Shimizu, Phys. Rev. A 2, 587 (1970).

11. Shirley, J. H., Phys. Rev. 138, B979 (1965).

12. Merzbacher, E., Quantum Mechanics (Wiley, New York, 1970).

13. Rabi, I. I., Phys. Rev. 51, 652 (1937).

14. Townes, C. H., and A. L. Schawlow, Microwave Spectroscopy (McGraw-Hill, New York, 1955).

15. Mizushima, M., Phys. Rev. 133, A414 (1964).

16. Bloch, F., and A. Siegert, Phys. Rev. 57, 522 (1940).

17. Stevenson, A. F., Phys. Rev. 58, 1061 (1940).

18. Shirley, J. H., J. Appl. Phys. 34, 783 (1963).

19. Salwen, H., Phys. Rev. 99, 1274 (1955).

20. Autler, S., and C. H. Townes, Phys. Rev. 100, 703 (1955).